START

PNL-7221
UC-702

Three-Dimensional Contaminant Plume Dynamics in the Vadose Zone: Simulation of the 241-T-106 Single-Shell Tank Leak at Hanford

J. L. Smoot
B. Sagar

January 1990

Prepared for the U.S. Department of Energy
under Contract DE-AC06-76RLO 1830

Pacific Northwest Laboratory
Operated for the U.S. Department of Energy
by Battelle Memorial Institute

Battelle

PNL-7221

THIS PAGE INTENTIONALLY
LEFT BLANK

DISCLAIMER

PACIFIC NORTHWEST LABORATORY
operated by
BATTELLE MEMORIAL INSTITUTE
for the
UNITED STATES DEPARTMENT OF ENERGY
under Contract DE-AC06-76RLO 1830

Printed in the United States of America

Available to DOE and DOE contractors from the
Office of Scientific and Technical Information, P.O. Box 62, Oak Ridge, TN 37831;
prices available from (615) 576-8401. FTS 626-8401.

Available to the public from the National Technical Information Service,
U.S. Department of Commerce, 5285 Port Royal Rd., Springfield, VA 22161.

NTIS Price Codes, Microfiche A01

Printed Copy

Price Code	Page Range	Price Code	Page Range
A02	1- 10	A15	326-350
A03	11- 50	A16	351-375
A04	51- 75	A17	376-400
A05	76-100	A18	401-425
A06	101-125	A19	426-450
A07	126-150	A20	451-475
A08	151-175	A21	476-500
A09	176-200	A22	501-525
A10	201-225	A23	526-550
A11	226-250	A24	551-575
A12	251-275	A25	576-600
A13	276-300	A99	601-Up
A14	301-325		

THIS PAGE INTENTIONALLY
LEFT BLANK

PNL-7221
UC-702

THREE-DIMENSIONAL CONTAMINANT PLUME DYNAMICS IN THE VADOSE ZONE: SIMULATION OF THE 241-T-106 SINGLE-SHELL TANK LEAK AT HANFORD

J. L. Smoot
B. Sagar

January 1990

Prepared for
the U.S. Department of Energy
under Contract DE-AC06-76RLO 1830

Pacific Northwest Laboratory
Richland, Washington 99352

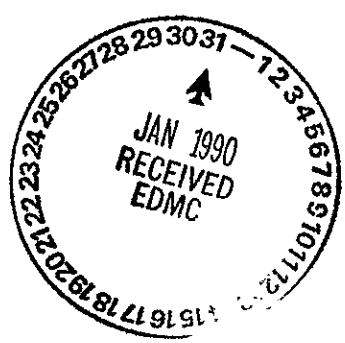

THIS PAGE INTENTIONALLY
LEFT BLANK

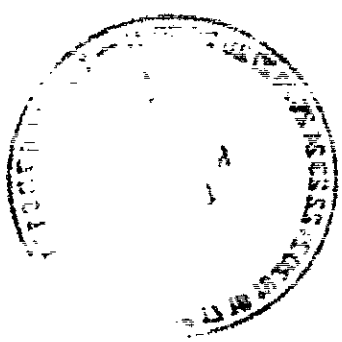

THE FOLLOWING

PAGES HAVE

BACKUPS

THIS PAGE INTENTIONALLY
LEFT BLANK

SUMMARY

Approximately 2,000 m^3 (115,000 gallons) of liquid containing radioactive and chemical wastes leaked from the 241-T-106 single-shell tank at the U.S. Department of Energy's Hanford Site in southcentral Washington in 1973. The leak discharged into the unsaturated, coarse-grained sediments of the Hanford formation which underlie the base of the tank. The extent of the contaminant plume in the vadose zone was estimated in 1973 and 1978 by gamma spectrometry in dry wells drilled to monitor the leak. The leak provides an excellent opportunity to test the applicability of the PORFLO-3 Version 1.0 computer code for studying flow and transport in the vadose zone.

The PORFLO-3 computer code was used to study plume migration for ^{106}Ru and ^{137}Cs. The flow and transport properties of the soils through which the plume has migrated are critical input data for the model but are not available. Consequently, information from a catalogue of Hanford Site soil properties was used. The transient magnitudes and locations of the plume were simulated in three dimensions.

Using viscosities and hydraulic conductivities for the tank fluid that are equal to that of water, the plume of ^{106}Ru simulated for 1973 was larger than that which was measured. By reducing the hydraulic conductivity for saturated conditions in the vertical direction by one-half, the dimensions of the simulated ^{106}Ru plume approximate those of the measured plume. Such reduction is justified because of the uncertainty inherent in the hydraulic conductivity data and because the tank fluid is more viscous than water. The plume of ^{137}Cs simulated for 1973 approximates that which was measured, assuming a reasonable distribution coefficient to account for the sorption of cesium by minerals of the Hanford formation.

Using the reduced vertical hydraulic conductivity, the migration of ^{106}Ru and ^{137}Cs was simulated for the time between 1973 and 1990. (The gamma spectrometry measurement in 1978 suggests that the ^{106}Ru did not move after 1973.) The plume simulated for 1978 and 1990, however, does not show this behavior; it appears to have expanded significantly since 1973. Because ^{106}Ru may have a small sorption coefficient, a simulation was made that

assumed a distribution coefficient of 0.5 for ruthenium. Use of this coefficient, however, did not result in a stationary ^{106}Ru plume; the simulated plume continued to expand after 1973.

This value is reasonable based on information in the literature. However, the use of the distribution coefficient did not accurately reproduce the lateral spreading of the observed plume, and the simulated plume expanded significantly after 1973.

The simulated plume of cesium for 1978 and 1990 did not move significantly from that measured and simulated for 1973. This static condition likely resulted from the sorption of cesium by minerals of the Hanford formation.

Simulations of the 241-T-106 tank leak indicate that PORFLO-3 Version 1.0 should be able to represent the transient behavior of a three-dimensional contaminant plume in the vadose zone. However, the quality of any simulation is directly proportional to the quality of the input data. The results of these simulations demonstrate the capability of the code; the results do not incorporate site-specific soil-moisture retention properties or site-specific radionuclide transport properties. These parameters should be measured. In addition, the 1989 distribution of the ^{106}Ru and ^{137}Cs plumes is unknown and should be measured. More data are needed for a comprehensive performance assessment analysis of the 241-T-106 tank leak. The results of this study indicate that such a performance assessment should be possible when site-specific data become available.

ACKNOWLEDGMENTS

The authors would like to thank Dr. Jerry Davis and Mr. Mike Connelly of Westinghouse Hanford Company (WHC) for technical support during the project. The authors would also like to thank WHC for computational support on the Hanford Cray X-MP/18.

THIS PAGE INTENTIONALLY
LEFT BLANK

CONTENTS

FIGURES

TABLES

1.0 INTRODUCTION

Chemical processing of spent nuclear fuel at the Hanford Site, located in southcentral Washington State, has resulted in the accumulation of large inventories of chemical, nuclear, and mixed wastes. From 1943 to 1964, a large part of this waste was stored underground in 149 single-shell tanks. One of the biggest leaks of single-shell tanks was detected on June 8, 1973, in the 241-T-106 single-shell tank located in the 200-West Area. Based on monitoring of liquid levels inside the tank, it was estimated that approximately 115,000 gallons of liquid were discharged to the soil (AEC-RL 1973; ARHCO 1973; Gillette 1973). Observation holes were drilled around the leak site to delineate the plume. Concentrations of radionuclide species were estimated from total gamma energy in the observation holes (ARHCO 1973). Measurements were made in 1973 and 1978 (Routson et al. 1979). In the present study, staff at the Pacific Northwest Laboratory,(a) in work funded by the U.S. Department of Energy (DOE) in support of Westinghouse Hanford Company, used field data to calibrate a complex numerical model of the T-106 site and then used the calibrated model to predict the present extent of the plume.

The computer code used in this study to model the 241-T-106 leak was PORFLO-3 Version 1.0 (Runchal and Sagar 1989; Sagar and Runchal 1989). PORFLO-3 is one of the hydrologic flow and transport computer codes that will be used to develop mathematical models from data collected at the Hanford Site and other DOE sites in order to evaluate the effectiveness of proposed remediation measures and the effects of new waste disposal activities. PORFLO-3 was designed to analyze flow and transport in complex, variably saturated, three-dimensional hydrogeologic settings. The 241-T-106 single-shell tank leak provides an opportunity to test the PORFLO-3 code; the ability to develop a model that approximates the extent of a measured plume engenders confidence in both the code and the data.

To obtain useful results, a large amount of data related to the leak and the site-specific hydrogeology is needed. Chapters 2, 3, and 4 discuss the

(a) The Pacific Northwest Laboratory is operated for the U.S. Department of Energy by Battelle Memorial Institute under Contract DE-AC06-76RLO 1830.

leak's history, the hydrogeology of the area in which the tank is located, and the nature of the leak. The conditions assumed in the model and the results of the model are discussed in Chapters 5 and 6. Chapter 7 summarizes the results and contains suggestions for future data collection.

2.0 BACKGROUND ON THE 241-T-106 LEAK

A total of 149 single-shell tanks are buried in the 200-East and 200-West Areas at Hanford (Figure 2.1). Sixty-six are located in the 200-East Area and 83 in the 200-West Area. The tanks are called single-shell tanks because they are constructed of concrete with a single-shell layer of carbon-steel lining. In contrast, tanks of more recent construction have two carbon-steel linings and are called double-shell tanks. The tanks are generally configured into "tank farms," which consist of groups of 6 to 18 buried tanks connected by pipes. Tank farms generally receive waste via pipe lines.

The wastes of a given tank farm were originally a product of the specific facilities and production processes being serviced by each tank farm. Both radioactive and chemical wastes were pumped into the tanks. In the early 1970s, the pumpable liquid wastes were pumped out and reprocessed to remove ^{90}Sr and ^{137}Cs that were generating high heat loads within the tanks. The wastes were then returned to the tanks with some mixing and likely misrouting during the process.

Single-shell tanks have dimensions ranging from 6 to 23 m (15 to 75 ft) in diameter and 6 to 15 m (15 to 50 ft) in height; they consist of buried concrete shells that are lined with a single layer of high carbon steel (Figure 2.2). The tanks are buried 40 to 70 m above the water table and are typically covered by several meters of overburden. Spatial relationships for the various sizes of tanks in each tank farm are shown in Figure 2.3. The 241-T-106 tank is a type II tank, having a diameter of 23 m (75 ft), a height of 8.5 m (28 ft), and a storage capacity of 2,000 m^3 (500,000 gal).

Thurman (1989) reported that 66 of the 149 single-shell tanks are assumed to have leaked, and Jensen et al. (1989) noted that the combined leak volume is about 2,800 m^3 (750,000 gal). The leaking single-shell tanks are listed in Table 2.1. Almost every tank farm is represented in the list. It is apparent that single-shell tank leakage is not an isolated problem. A more comprehensive analysis at a scale larger than the single tank scale used in the present analysis may be required to assess the effects of the leaks.

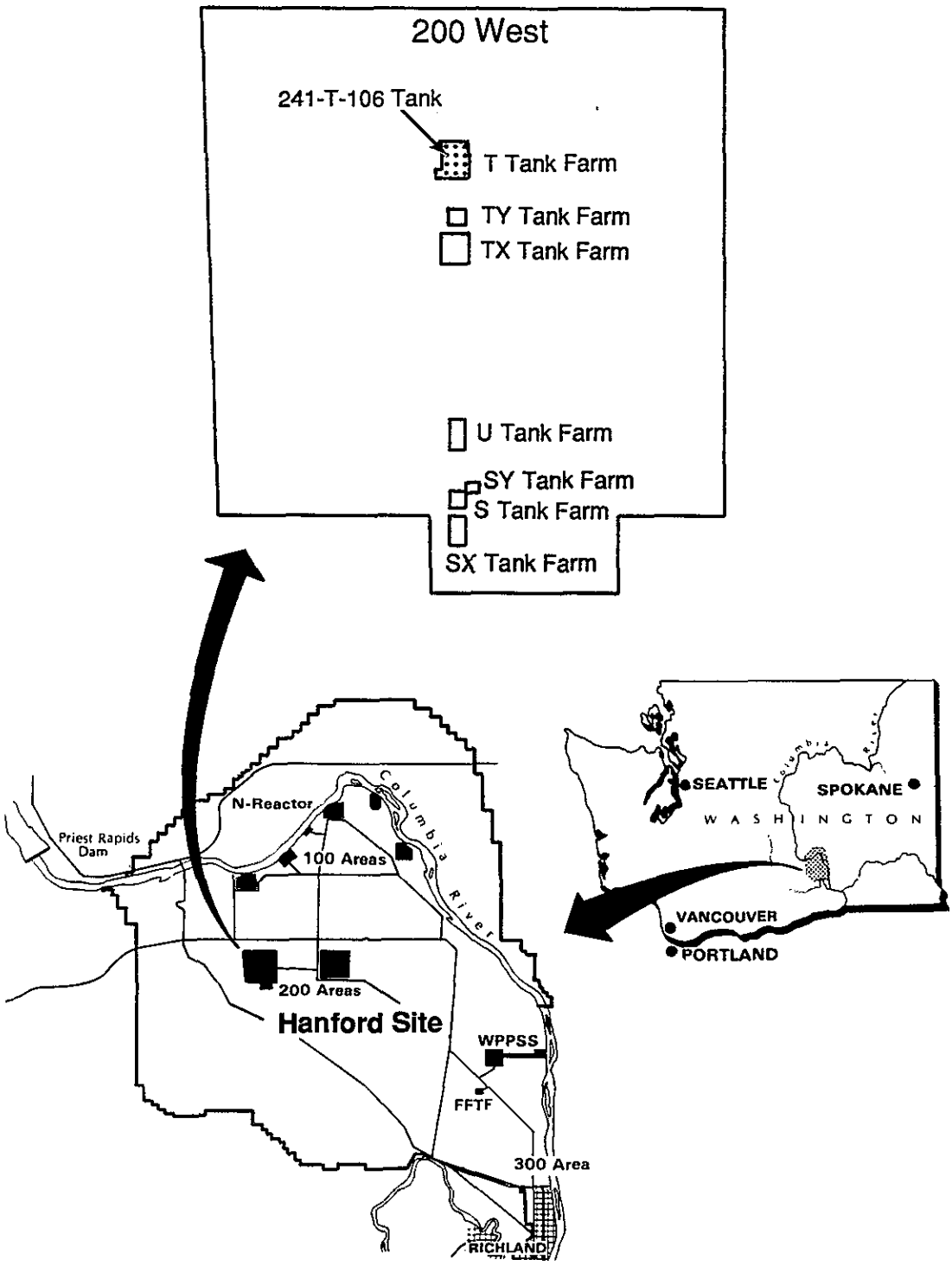

FIGURE 2.1. Location of Hanford T Tank Farm

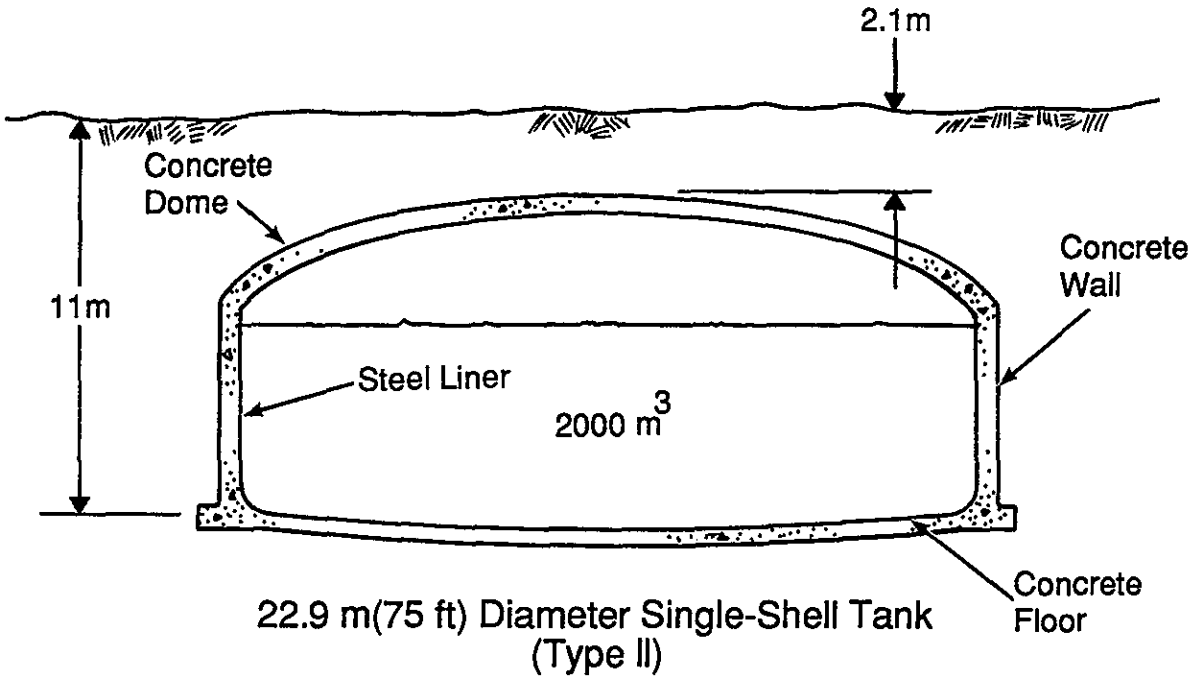

FIGURE 2.2. Design of the 241-T-106 Single-Shell Tank (after DOE 1987)

ARHCO (1973) and Routson et al. (1979) described the 241-T-106 tank leak in detail, and their work provides important information for this modeling analysis.

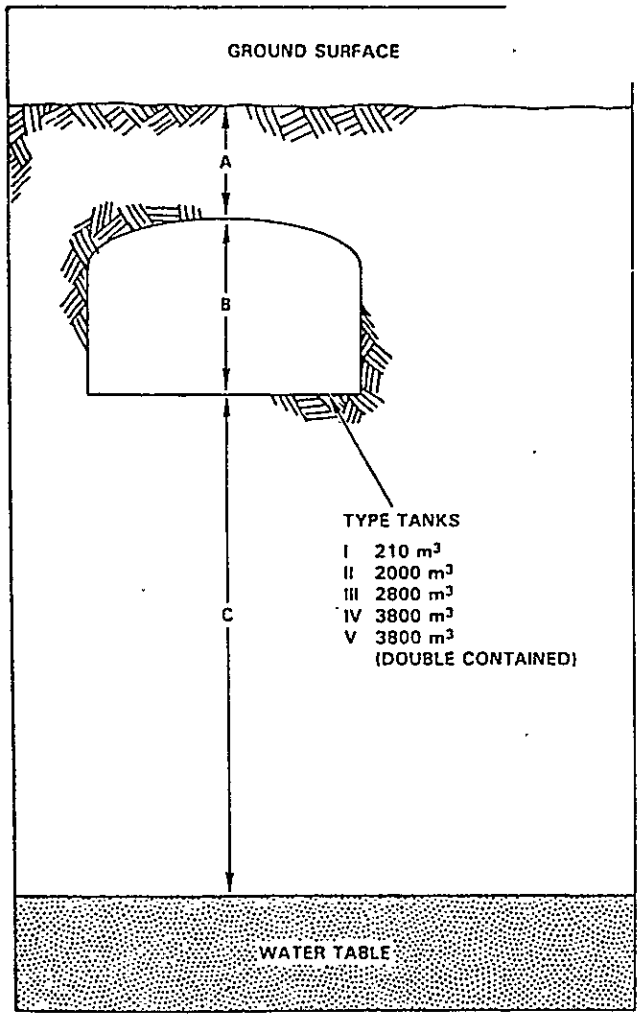

	NUMBER OF TANK TYPES					DIMENSIONS (m)		
TANK FARM	I	II	III	IV	V	A	B	C (APPROX)
A				6		2.3	14.3	70.1
AX				4		2.3	14.3	65.8
AY					2	2.1	14.9	65.8
AZ					2	2.1	14.9	59.4
B	4					1.8	6.1	64.3
B		12				1.8	8.5	61.9
BX		12				2.7	9.8	66.4
BY			12			2.4	11.9	60.0
C	4					1.8	6.1	69.5
C		12				2.7	8.5	66.1
S			12			2.4	11.9	43.9
SX				15		2.3	14.3	43.0
T	4					1.8	6.1	53.9
T		12				2.7	8.5	50.6
TX			18			2.4	11.9	51.2
TY			6			2.4	11.9	46.6
U	4					1.8	6.1	53.6
U		12				2.7	8.5	50.3
AW					6	2.1	14.9	69.5
AP					8	2.5	14.9	67.4
AN					7	2.1	14.9	63.4
SY					3	2.1	14.9	42.1

FIGURE 2.3. Placement of the 241-T-106 Single-Shell Tank (after DOE 1987)

TABLE 2.1. Single-Shell Tank Assumed Leakers (after Thurman 1989)

Tank Number	Year of Construction	Year Removed[a] From Service	Operating Capacity, gal
200-EAST AREA: 32 Tanks			
Waste Management Area B-BX-BY			
241-B-101	1943-1944	1974	500,000
241-B-103	1943-1944	1977	500,000
241-B-105	1943-1944	1972	500,000
241-B-107	1943-1944	1969	500,000
241-B-110	1943-1944	1971	500,000
241-B-111	1943-1944	1976	500,000
241-B-112	1943-1944	1977	500,000
241-B-201	1943-1944	1971	55,000
241-B-203	1943-1944	1977	55,000
241-B-204	1943-1944	1977	55,000
241-BX-101	1946-1947	1972	500,000
241-BX-102	1946-1947	1971	500,000
241-BX-108	1946-1947	1974	500,000
241-BX-110	1946-1947	1977	500,000
241-BX-111	1946-1947	1977	500,000
241-BY-103	1948-1949	1973	750,000
241-BY-105	1948-1949	1974	750,000
241-BY-106	1948-1949	1977	750,000
241-BY-107	1948-1949	1974	750,000
241-BY-108	1948-1949	1972	750,000
Waste Management Area C			
241-C-101	1943-1944	1970	500,000
241-C-110	1943-1944	1976	500,000
241-C-111	1943-1944	1978	500,000
241-C-201	1943-1944	1977	55,000
241-C-202	1943-1944	1977	55,000
241-C-203	1943-1944	1977	55,000
241-C-204	1943-1944	1977	55,000
Waste Management Area A-AX			
241-A-103	1954-1955	1980	1,000,000
241-A-104	1954-1955	1975	1,000,000
241-A-105	1954-1955	1963	1,000,000
241-AX-102	1963-1964	1980	1,000,000
241-AX-104	1963-1964	1978	1,000,000

(a) The last year the tank was capable of receiving waste; actual date of last waste receipt may have been earlier.

TABLE 2.1. (contd)

Tank Number	Year of Construction	Year Removed(a) From Service	Operating Capacity, gal
200-WEST AREA: 34 Tanks			
Waste Management Area T			
241-T-103	1943-1944	1974	500,000
241-T-106	1943-1944	1973	500,000
241-T-107	1943-1944	1976	500,000
241-T-108	1943-1944	1974	500,000
241-T-109	1943-1944	1974	500,000
241-T-111	1943-1944	1974	500,000
241-TX-105	1947-1948	1977	750,000
241-TX-107	1947-1948	1977	750,000
241-TX-110	1947-1948	1977	750,000
241-TX-113	1947-1948	1971	750,000
241-TX-114	1947-1948	1971	750,000
241-TX-115	1947-1948	1977	750,000
241-TX-116	1947-1948	1969	750,000
241-TX-117	1947-1948	1969	750,000
241-TY-101	1951-1952	1973	750,000
241-TY-103	1951-1952	1973	750,000
241-TY-104	1951-1952	1974	750,000
241-TY-105	1951-1952	1980	750,000
241-TY-106	1951-1952	1959	750,000
Waste Management Area U			
241-U-101	1943-1944	1960	500,000
241-U-104	1943-1944	1951	500,000
241-U-110	1943-1944	1975	500,000
241-U-112	1943-1944	1970	500,000
Waste Management Area S-SX			
241-S-104	1950-1951	1968	750,000
241-SX-104	1953-1954	1980	1,000,000
241-SX-107	1953-1954	1964	1,000,000
241-SX-108	1953-1954	1962	1,000,000
241-SX-109	1953-1954	1965	1,000,000
241-SX-110	1953-1954	1976	1,000,000
241-SX-111	1953-1954	1974	1,000,000
241-SX-112	1953-1954	1969	1,000,000
241-SX-113	1953-1954	1958	1,000,000
241-SX-114	1953-1954	1972	1,000,000
241-SX-115	1953-1954	1965	1,000,000

(a) The last year the tank was capable of receiving waste; actual date of last waste receipt may have been earlier.

3.0 HYDROGEOLOGY

The hydrogeology of the area of the 241-T-106 tank is described in terms of the stratigraphy of the area, the unconfined aquifer, and water movement (moisture retention and recharge) through the unsaturated zone.

3.1 STRATIGRAPHY OF THE UNSATURATED ZONE

The single-shell tanks are buried in generally coarse-grained sediments of Pleistocene and Holocene age that overlie the Columbia River basalts in the Pasco Basin. The sediments overlying the basalts are divided into the Ringold Formation and the overlying Hanford formation, separated by a distinct unit of Plio-Pleistocene age. The Ringold Formation is of Pliocene age, and is generally coarse-grained, but with occasional thin layers of fine sand or silt with small amounts of clay. Caliche is observed in both the basal Ringold and the Plio-Pleistocene unit. The Hanford formation is of Pleistocene age and consists of a very coarse-grained flood facies called the Pasco Gravels and a finer-grained slackwater facies called the Touchet Beds.

Tallman et al. (1979), Bjornstad (1983), DOE (1987), and more recently Jensen et al. (1989), Last and Bjornstad (1989), and Last et al. (1989) describe the geology of the unconsolidated sediments in the vicinity of the 200-West Area. In general, the vadose zone consists of a portion of the thick, relatively coarse-grained, elastic sediments of the middle Ringold Formation, overlain by the finer-grained, elastic sediments of the upper Ringold Formation and the Plio-Pleistocene unit, overlain in turn by the coarser-grained sands and gravels of the Hanford formation, which are exposed at the surface. The upper 10 to 20 m of the Hanford formation were locally excavated and back-filled during installation of the single-shell tanks. In the remainder of this report, this zone is described as backfill to distinguish it from undisturbed Hanford formation.

Price and Fecht (1976) and Fecht and Price (1977) focus on the geology of the 241-T Tank Farm. Their 1976 report provides the most detailed geologic interpretation of the hydraulic (hydrologic) properties around the T-106 tank (see Figure 3.1). The water table is located within a thick sequence of sandy gravel that probably is part of the middle member of the

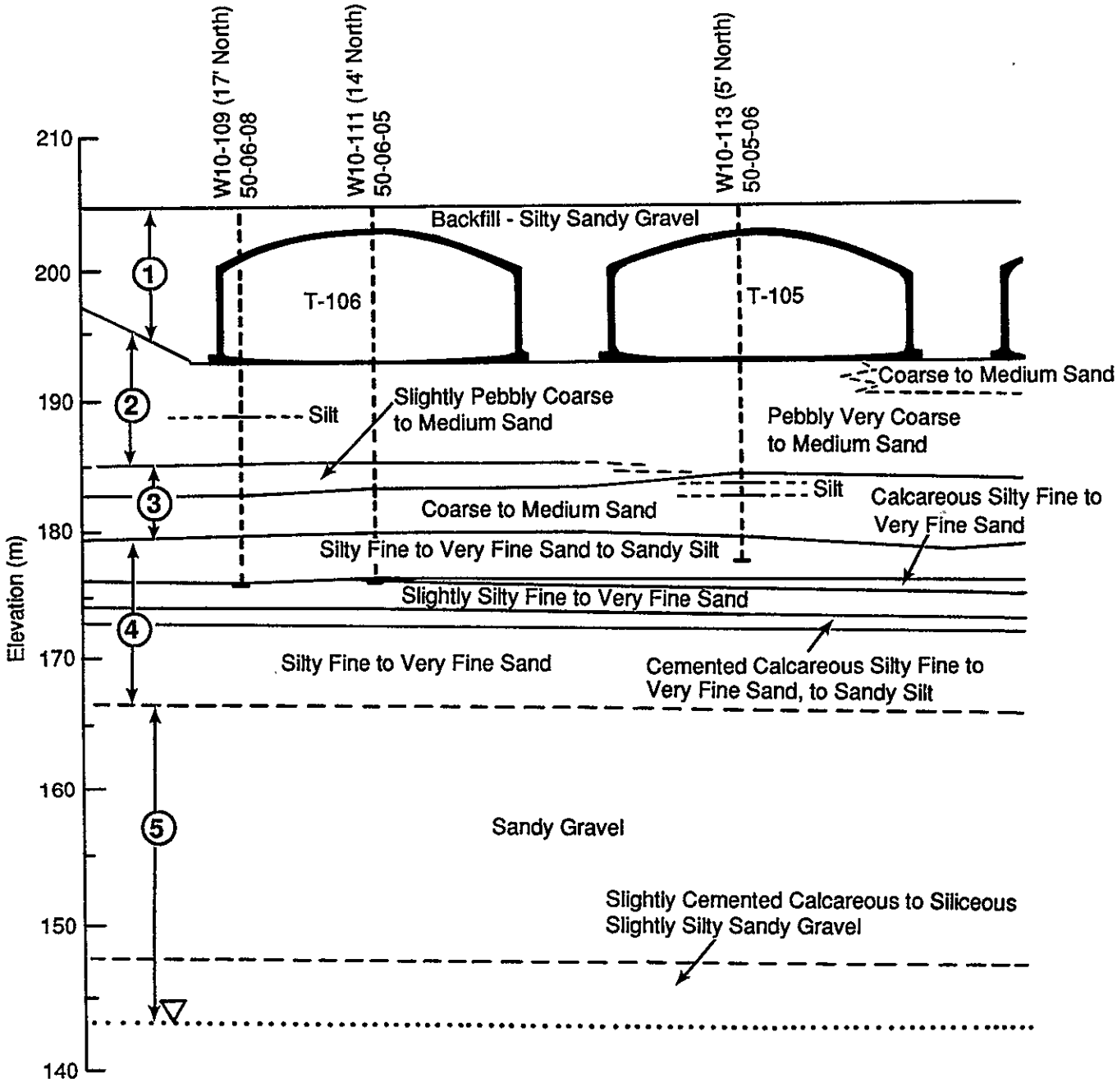

FIGURE 3.1. Stratigraphy of the T Tank Farm (after Price and Fecht 1976)

Ringold Formation. These coarse-grained sediments are overlain by about 14 m of fine-grained sediments that probably are part of the upper Ringold Formation and at least a portion of the Plio-Pleistocene unit. These sediments consist of layered silty, fine to very-fine-grained sand with

intercalated, calcareous zones. At an elevation of about 173 m, or approximately 30 m below the surface, the sediments appear to be highly cemented by caliche.

Overlying the fine-grained sediments are about 4 m of somewhat coarser-grained material consisting of coarse to medium-grained sand with some pebbles in the upper portion. This zone may contain sediments from both the upper Plio-Pleistocene unit and the lower portion of the Hanford formation. Above this zone, about 8 m of the pebbly, very coarse to medium-grained sands of the Hanford formation extend to the base of the single-shell tanks. The backfill, silty, sandy, gravel, composes the remaining 12 m of sediments to the surface. The backfill was derived from the excavated material.

Based primarily on the work of Price and Fecht (1976), but in general agreement with more recent work, five stratigraphic subdivisions may be inferred for the unsaturated zone in the vicinity of the 241-T Tank Farm. These zones are shown in Figure 3.2. The total section is 61 m thick. Beginning at the water table, the vadose zone consists of about 23 m of sandy gravel overlain by 14 m of calcareous, silty fine-grained to very fine sand, which may include a caliche layer. Above this is 4 m of coarse to medium-grained sand overlain by 8 m of pebbly, very coarse to medium-grained sand, which in turn is overlain by 8 m of pebbly, very coarse to medium-grained sand, and finally capped by about 12 m of silty, sandy, gravelly backfill.

3.2 UNCONFINED AQUIFER

The unconfined aquifer in the vicinity of the 241-T-106 tank is contained within the unconsolidated sediments of the middle, lower, and basal members of the Ringold Formation; the underlying Columbia River basalts are assumed to form the base of this aquifer. Water levels in the unconfined aquifer are well documented for recent years. Ground water flows generally toward the Columbia River. Depths to water are commonly on the order of 60 to 80 m.

There may be some hydraulic communication between confined aquifers in the basalt and the unconfined aquifer, although the direction and magnitude

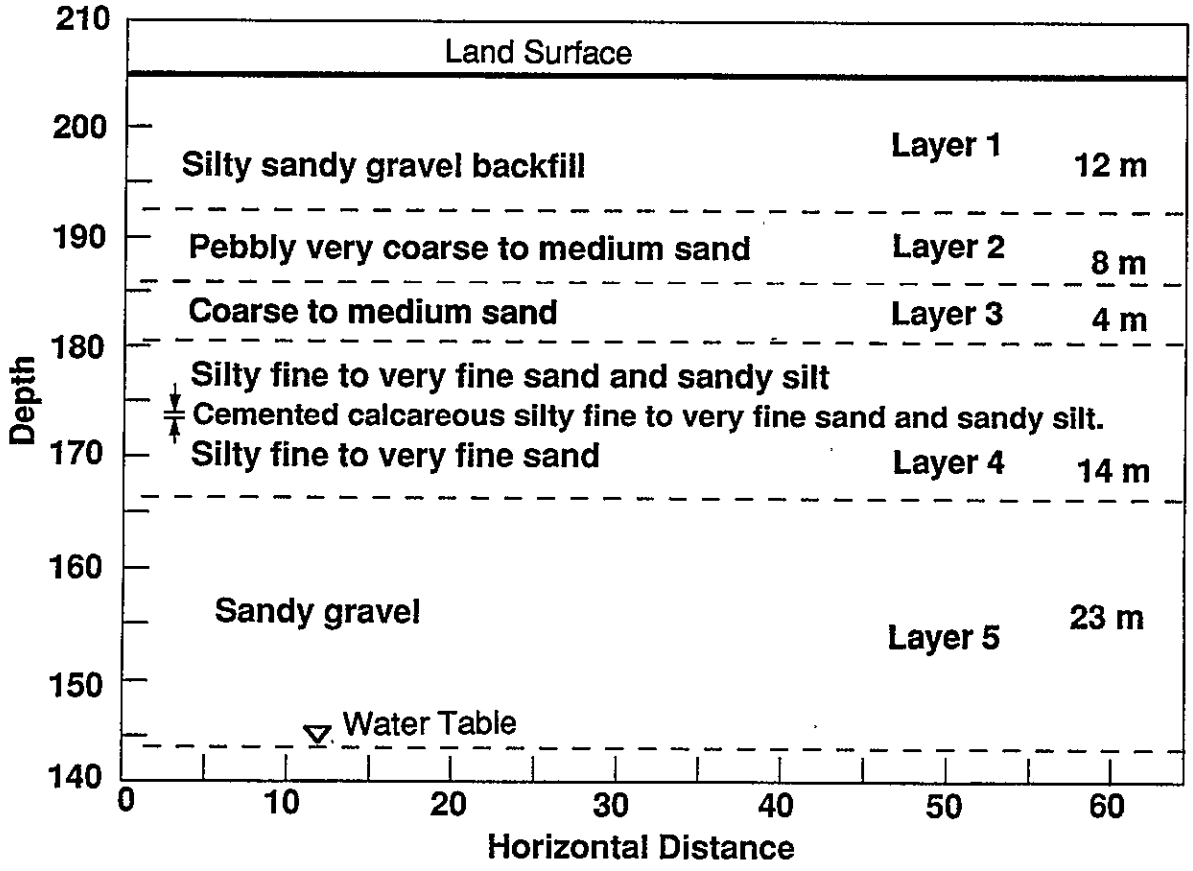

FIGURE 3.2. Textures and Thicknesses of the Five Major Stratigraphic Zones at the T Tank Farm

of any such flow are yet to be documented. Hydraulic conductivity and saturated thickness of the unconfined aquifer vary considerably across the site, yet produce a relatively constant distribution of transmissivity.

3.3 WATER MOVEMENT THROUGH THE UNSATURATED ZONE

3.3.1 Deep Percolation (Recharge)

Water from precipitation infiltrating past the root zone will percolate downward through the unsaturated zone. This water constitutes recharge to the unconfined aquifer. The percentage of precipitation that becomes available for recharge is a subject of continued research at Hanford. Gee (1987) notes that recharge rates at the Hanford Site may vary from zero to more than the average annual precipitation at specific locations. He notes

that measured differences in drainage in a wide variety of lysimeters installed at the Hanford Site may be attributable to differences in plant cover. Maximum drainage tends to occur in areas that have no plant cover, such as the bare, gravelled surface maintained at the T Tank Farm. He notes that at areas such as the tank farm sites, where the surface is gravelly, "most of the annual precipitation can be expected to drain through the gravel and be available for recharge." The average annual precipitation at the Hanford Site is about 15 cm/yr; consequently, the surface of the T Tank Farm may allow a significant portion of this water to become available for recharge.

The manner in which the tanks alter the flow field may also be an important factor with respect to recharge. The tanks can be expected to divert infiltrating water that encounters their domed tops. This water would then percolate along the sides of the tanks, producing a ring of soil beneath the tanks that may be of a relatively higher moisture content and, therefore, higher hydraulic conductivity. Philip et al. (1989) report similar phenomena for smaller-scale features in the unsaturated zone. However, measurements to support this hypothesis for the tank farms have not yet been made.

3.3.2 Moisture Retention Characteristics of the Vadose Zone Sediments

Moisture retention properties of soils and sediments are critical hydrologic parameters for analyzing water flow for unsaturated conditions but have not been measured for the soils at the 241-T Tank Farm. For the purposes of this analysis, soil moisture retention characteristics were estimated using a qualitative comparison of soil textural and stratigraphic properties with catalogues of data that document these characteristics for specific Hanford Site locations. Details of these characteristic curves are provided in Section 5.4.

THIS PAGE INTENTIONALLY
LEFT BLANK

4.0 DESCRIPTION OF THE 241-T-106 SINGLE-SHELL TANK LEAK

Routson et al. (1979) provide a detailed chronology of the 241-T-106 tank leak. Leakage began on or about April 20, 1973, when the tank was filled with reprocessed wastes. Leakage stopped on June 10, 1973, when the pumpable liquid contents of the tank were removed. The total duration of the leak was approximately 52 days, during which 115,000 gallons of supernate were lost from the tank.

The radionuclide inventory of the supernate solution within the tank is shown in Table 4.1. Most of the inventory consists of $^{144}Ce/^{144}Pr$, ^{137}Cs, $^{89}Sr/^{90}Sr$, and $^{106}Ru/^{106}Rh$, with lesser amounts of the other radionuclides. With the exception of $^{106}Ru/^{106}Rh$, the inventory is characterized by long half-lives and high sorption coefficients. The inventory in Table 4.1 corresponds to about 2.67×10^5 Ci of ^{106}Ru and 3.85×10^4 Ci of ^{137}Cs. This compares to 4×10^4 Ci of ^{137}Cs reported by the U.S. Energy Research and Development Agency (1975). Ruthenium-106 has a half-life of about 1 year, and sorption coefficients are generally small. Consequently, the movement of ^{106}Ru should be essentially concurrent with the fluid front.

The tank leak apparently occurred on the southeast side of the tank. The contaminant plume is centered around this portion of the tank. Figure 4.1 shows both a plan view and a vertical cross-sectional view of the plume in the summer of 1973, after the leak had been detected and the tank pumped out. Contaminant transport is shown for ^{106}Ru, ^{144}Ce, and ^{137}Cs. Ruthenium-106 is the most mobile of the three and had traveled the farthest, while ^{137}Cs is the least mobile and was contained within a small zone around the base of the tank. The configuration of the ^{106}Ru plume appears to be approximately circular, with a radius of about 15 to 20 m in plan view and a maximum depth of penetration of about 20 m. Figure 4.2 shows the horizontal and vertical distribution of ^{106}Ru for several isopleths. The figure reveals a relatively steep distribution front both laterally and vertically.

Figure 4.3 shows the isopleths measured for ^{106}Ru 1-μCi/L in 1973 and 1978. From Figure 4.3, the ^{106}Ru 1-μCi/L isopleth does not appear to have migrated during this period. Because of its relatively short (1-yr) half-life, the ^{106}Ru would decay from the 2.7×10^{11} μCi leaked from the tank in

TABLE 4.1. Radionuclide Inventory of the 241-T-106 Tank Supernatant Solution (after Routson et al. 1979)

Radioactive Component	Ci/l	Ci/gal
Cerium-144/Praseodymium-144	1.18×10^4	4.48×10^4
Cesium-137	8.85×10^4	3.35×10^5
Europium-155	1.69×10^3	6.40×10^3
Cesium-134	1.32×10^3	5.00×10^3
Antimony-125	1.12×10^4	4.24×10^3
Strontium-89/Strontium-90	2.98×10^4	1.13×10^5
Ruthenium-106/Rhodium-106	6.12×10^5	2.32×10^6
Plutonium-239	9	34
Plutonium-240	2	8
Americium-241	2	6

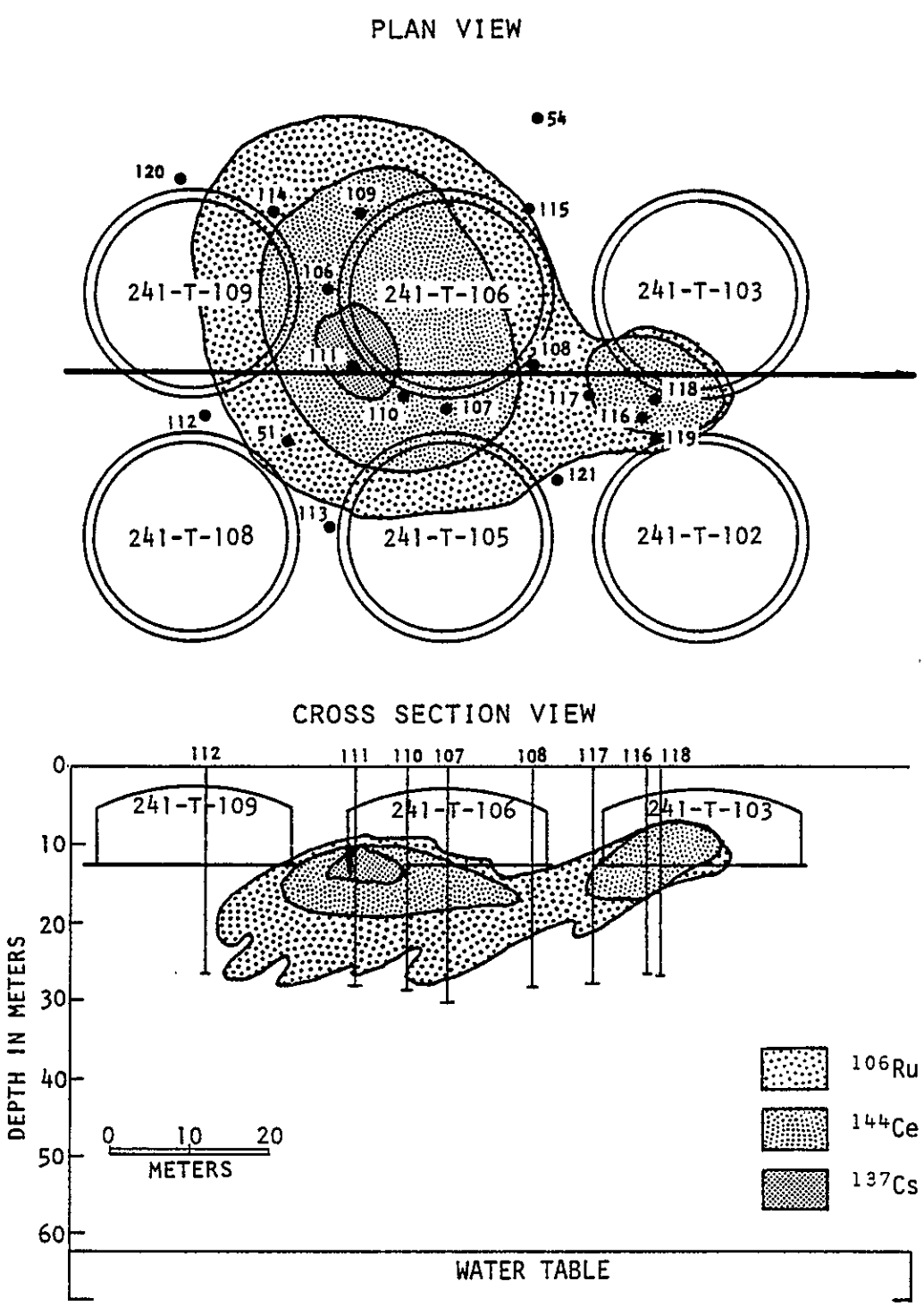

FIGURE 4.1. Plan and Vertical Cross-Sectional Views of the ^{137}Cs, ^{137}Ce, and ^{106}Ru 1-μCi/L Volumetric Isopleths in 1973 (after Routson et al. 1979)

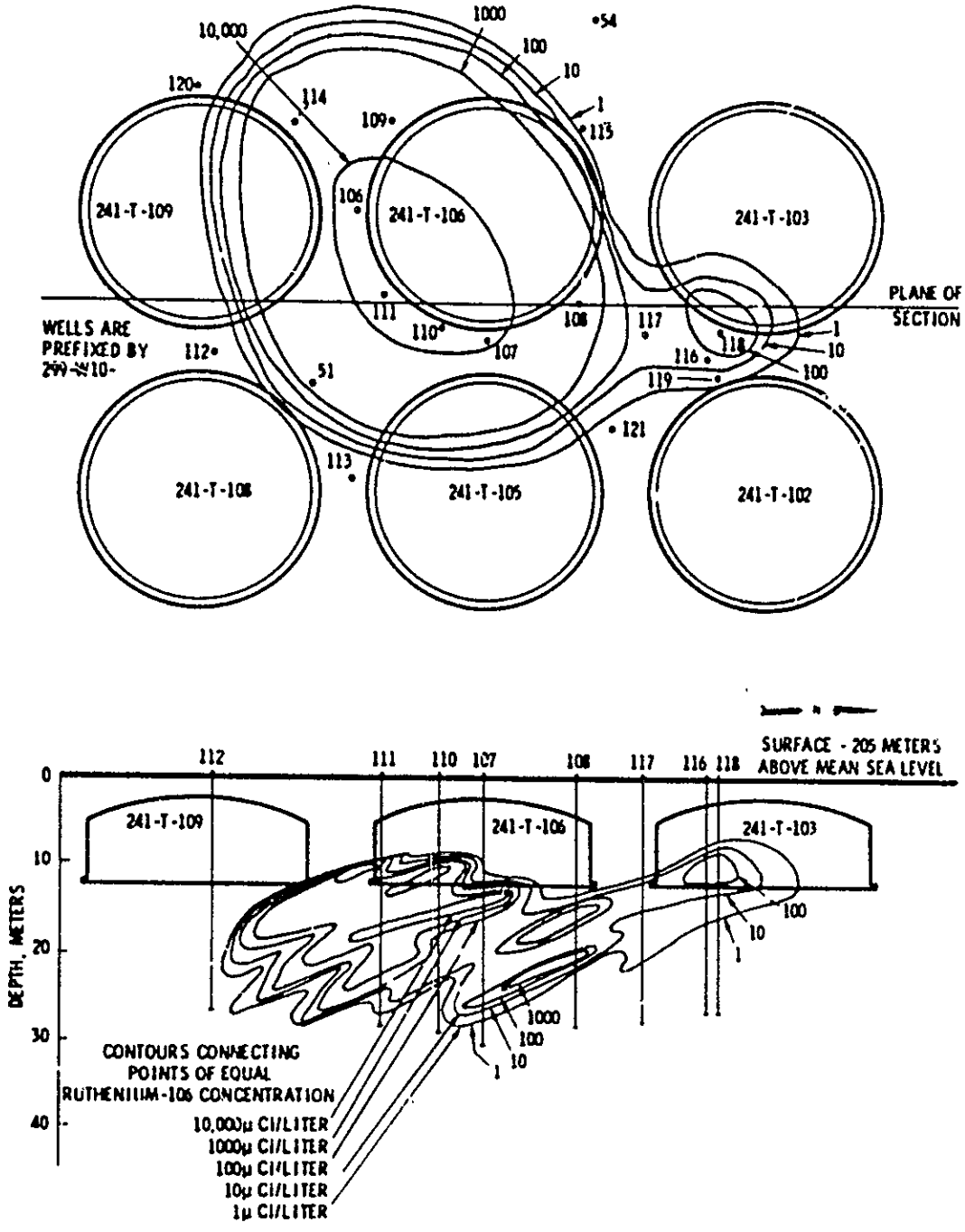

FIGURE 4.2. Vertical Cross Section of the ^{106}Ru Plume (after ARHCO 1973)

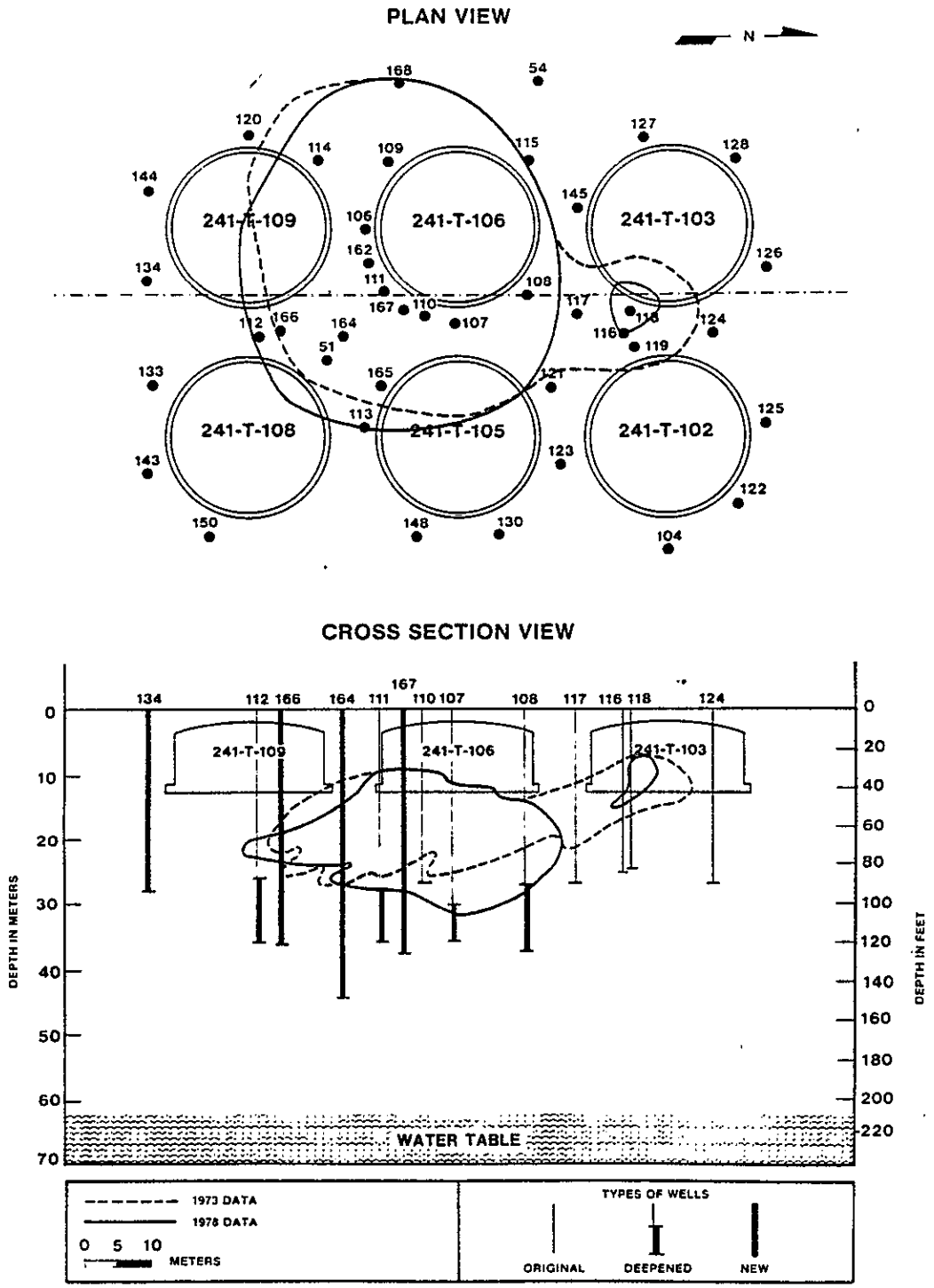

FIGURE 4.3. Plan and Vertical Cross-Sectional Views of the ^{137}Cs, ^{137}Ce, and ^{106}Ru 1-μCi/L Volumetric Isopleths in 1978 (after Routson et al. 1979)

1973 to about 8.4 x 10^9 μCi in 1978. However, the decay process alone is not sufficient to explain the measured stasis of the 1-μCi/L isopleth of ^{106}Ru in 1978. As will be indicated later, model simulations fail to reproduce this stasis.

5.0 NUMERICAL SIMULATION

No computer simulation of the 241-T-106 tank leak has previously been published. A simulation with axisymmetric geometry and assumed tank-leak conditions was made by Rockwell Hanford Operations staff, but that study was never published. Most simulations of fluid-flow and contaminant transport in the vadose zone of the Hanford Site have been one-dimensional. In contrast, ground-water flow and contaminant transport in the unconfined aquifer have been extensively simulated (Evans et al. 1988).

5.1 CONCEPTUAL MODEL

Leakage from the T-106 tank appears to have been contained within the unsaturated zone. Consequently, the object of this analysis was to focus on contaminant transport through the unsaturated zone. The major stratigraphic subdivisions in the vicinity of the T-106 tank are described in Section 3.1 (see Figure 3.2). These subdivisions are incorporated into the domain of the three-dimensional model. Approximately 115,000 gallons of supernate leaked into this soil column during an approximate 52-day period in the late spring of 1973. A ^{106}Ru plume developed by the summer of 1973, with a horizontal radius of about 15 to 20 m and extending to a depth of about 20 m below the base of the tank.

In the horizontal plane, the model domain encompasses an area of about 6,000 m^2 centered approximately on the T-106 tank. The model extends vertically about 60 m to the water table. At this scale, each stratigraphic subdivision within the domain is assumed to be of constant thickness. No flow is allowed across the vertical (sides and ends) boundaries of the domain. Thus, at the scale of the model domain, the flow is vertical. However, locally in the vicinity of the leak, the flow is fully three-dimensional. The water table forms the lower boundary for the model. The pressure at this boundary is assumed to remain fixed at the atmospheric value. A uniform infiltration rate is applied to the upper surface of the model. The tank itself is represented as an impervious group of grid cells.

This treatment allows the infiltrating water to be diverted around the tank. Thus, in a local zone around the perimeter of the tank, the volumetric flux may be significantly enhanced.

5.2 DISCRETIZATION

The three-dimensional domain is a region of 3.7×10^5 m^3, having dimensions of 88 x 68 x 62 m. This domain was discretized into a 24 x 15 x 33 m grid containing 11,880 cells. The discretization is shown in Figure 5.1 for the x, y, and z directions. A variable grid spacing is used in all three dimensions. The grid mesh in the x and y (horizontal) directions is finest (2 m) near the middle of the domain, where the T-106 tank is located just beneath the surface, and coarsens toward the edges of the model domain.

The model domain is discretized vertically in the z (vertical) direction, from the surface down to the water table. Each of the five major stratigraphic subdivisions is further subdivided, resulting in a total of 33 cells in the z direction. The grid size varies in the z direction from 0.5 m near the base of the T-106 tank to 8 m near the water table.

5.3 BOUNDARY AND INITIAL CONDITIONS

The boundary conditions are shown in Figure 5.2. The vertical boundaries around the perimeter of the domain were specified to be no-flow boundaries, based on the assumption of predominantly vertical flow within the unsaturated zone. The upper boundary at the ground surface was specified to be an infiltration-source boundary. An infiltration rate of 0.05 m/yr was simulated. Although Gee's (1987) preliminary results indicate that the rate of infiltration of meteoric water for an unvegetated, gravel-covered surface may be higher, 0.05 m/yr was used as an initial estimate. This value was estimated as approximately 30% of precipitation. As noted in Section 3.3.1, recharge to the unconfined aquifer may vary from zero to greater-than-average annual precipitation at specific locations of the Hanford Site. The lower boundary at the water table was assumed to be at atmospheric pressure.

Initial conditions were set for hydraulic head and radionuclide concentration throughout the model domain. Initially, the matric potential within the unsaturated sediments was assumed to be in equilibrium with a

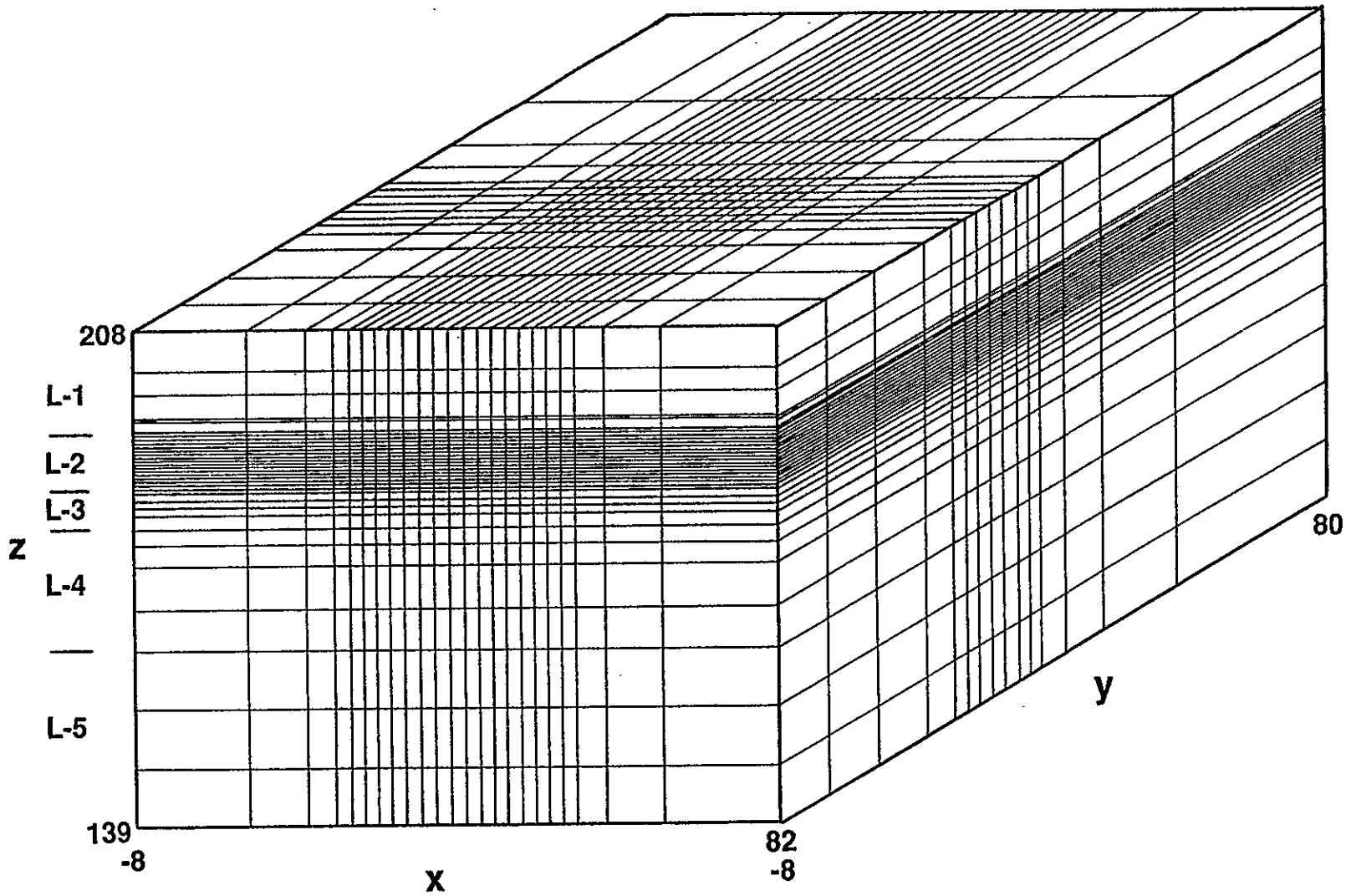

FIGURE 5.1. Discretization of the Three-Dimensional Model

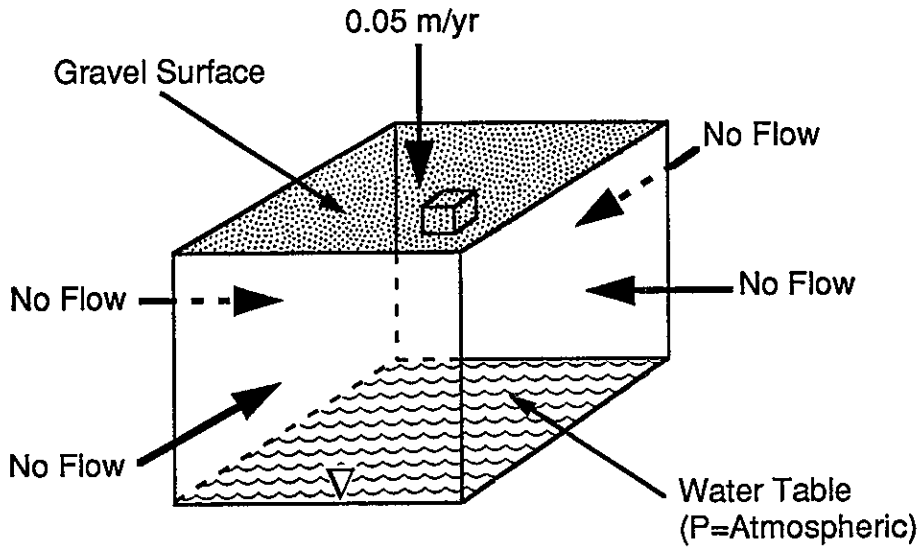

FIGURE 5.2. Boundary Conditions of the Three-Dimensional Model

constant 0.05 m/yr infiltration rate. By assuming approximate unit gradient conditions over a unit area, the hydraulic conductivity becomes approximately equal to the infiltration rate and the matric potential may be estimated for each of the five stratigraphic units from the assigned moisture characteristic curves. The initial condition total hydraulic head was calculated at each node by adding the corresponding elevation (or gravity head) to the matric potential.

The starting time of the simulation was immediately before the start of the leak. The initial concentration of radionuclides was set equal to zero throughout the soil column. Because the tank is impervious, the radionuclide concentrations inside the tank are immaterial.

5.4 SOIL HYDRAULIC AND TRANSPORT PROPERTIES

Although directly measured soil properties for the 241-T-106 site are not currently available, several small data catalogues are available describing moisture retention data for soil samples obtained elsewhere at the Hanford Site. The only soil-property data for the single-shell tank farm are described by Sewart et al. (1987). These data are for five soil samples collected during excavation of the 210-AP Tank Farm in the 200-East Area.

The textural descriptions of the samples (Sewart et al. 1987) were compared with descriptions of the five stratigraphic units identified at the T Tank Farm. This comparison is shown in Table 5.1. The analogues were obtained by using a data catalogue containing only a limited amount of soil data. The absence of data specific to the 241-T-106 tank site introduced an undetermined amount of uncertainty into the simulation results.

The moisture retention curves for the five stratigraphic subdivisions in the model are shown in Figures 5.3 through 5.7. The curves show that the soils exhibit a relatively wide range of properties. The corresponding unsaturated hydraulic conductivities (K) for isotropic conditions as a function of volumetric moisture contents (θ_S) are also shown for each stratigraphic unit.

An important factor in the simulation is the representation of the tank in the subsurface as a solid object that would divert infiltration. Because the PORFLO-3 code does not allow the assignment of inactive (no-flow) cells within the grid mesh, the tank must be represented using soil properties. The various coefficients used to represent the tank as an essentially impervious object are shown below:

- $n = 0$ where n is porosity
- $K_X = K_Y = K_Z = 1 \times 10^{-30}$ where K is hydraulic conductivity
- $S_S = 0$ where S_S is the specific storage
- $\alpha_L = \alpha_T = 1 \times 10^{-30}$ where α_L is longitudinal dispersivity and α_T is transverse dispersivity
- $C = C_{max}$ where C is concentration.

The porosity is set to zero. The specific storage (S_S) is also set to zero, and the hydraulic conductivity (K_X) is given a nominal but nonzero value.

Transport coefficients were assumed for each of the five stratigraphic units. For all units, the Fickian molecular diffusion coefficient (D) was held constant at 1×10^{-5} m^2/day and longitudinal and transverse dispersivity at 1.0 m and 0.1 m, respectively. For those model simulations that address retardation, a distribution coefficient of 5×10^{-7} m^3/g (0.5 mL/g) was used for ^{106}Ru and 1×10^{-4} m^3/g (100.0 mL/g) for ^{137}Cs. Continued work is needed to quantify contaminant transport properties of Hanford Site soils; the values used in the simulation were only estimates.

TABLE 5.1. T Tank Farm Soil Properties and the Corresponding 241-AP Soil Catalogue Properties Used in the Modeling Analysis

T Tank Farm Soil Properties	Corresponding 241-AP Tank Farm Excavation Soil Description (after Sewart et al. 1987 p. 5.7)
Layer 1: Silty sandy gravel backfill	AP Soil 1: Sandy gravel, Unconsolidated, horzontally bedded, very coarse sand with very fine to very coarse pebbles
Layer 2: Pebbly very coarse to medium sand	AP Soil 2: Sand. Well-consolidated, horizontally bedded, medium to coarse sand
Layer 3: Coarse to medium sand	AP Soil 4: Gravelly sand. Very unconsolidated coarse sand with pebbles and small cobbles
Layer 4: Silty, fine to very fine sand and sandy silt with calcareous, cemented sublayers	AP Soil 5: Silty sand. Very well consolidated, horizontally bedded very find sand and silt
Layer 5: Sandy gravel	AP Soil 1: Sandy gravel. Unconsolidated, horizontally bedded, very coarse sand with very fine to very coarse pebbles

Stratigraphic Subdivisions 1,5

AP-1G

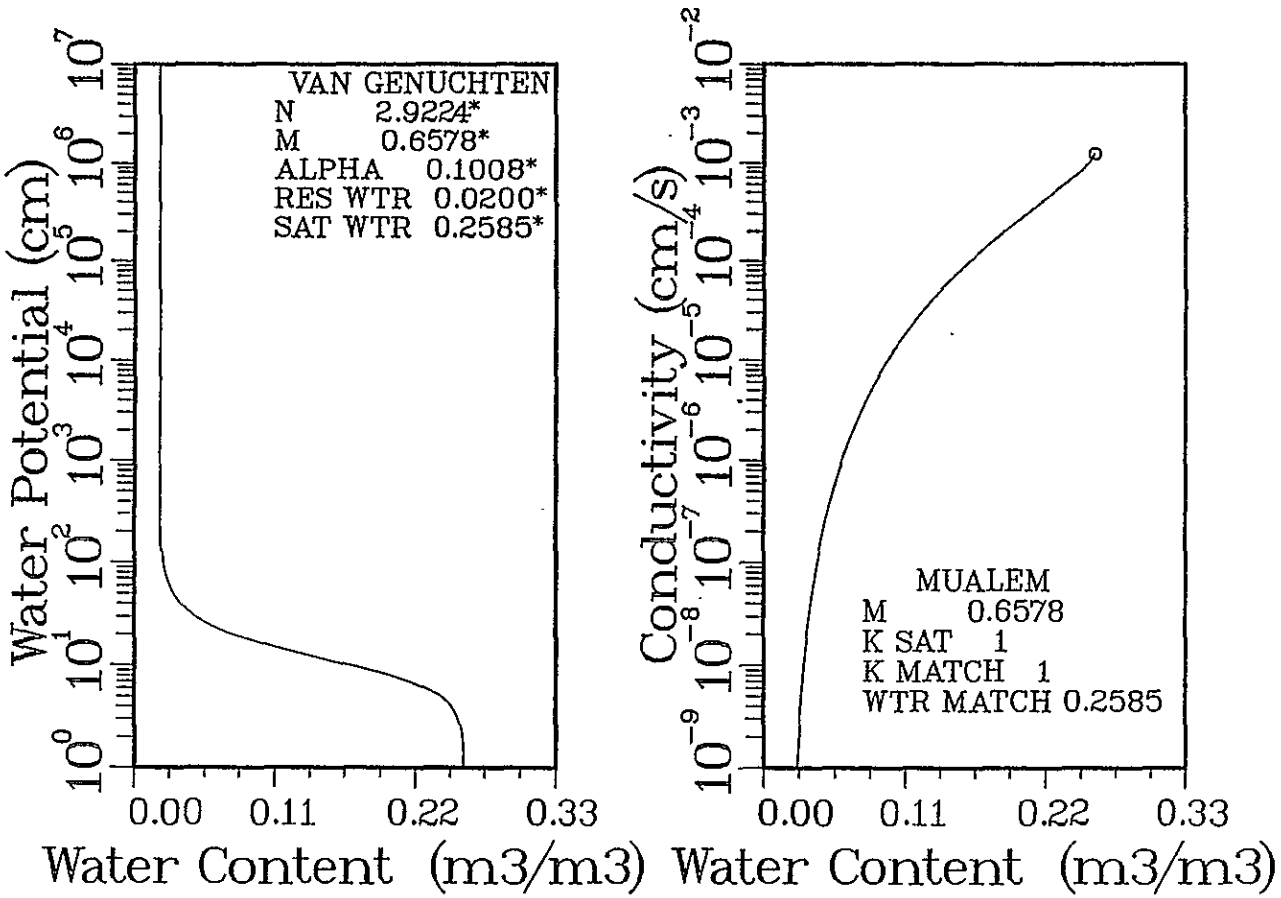

FIGURE 5.3. Moisture Retention Curves Identified for Stratigraphic Units One and Five at the T Tank Farm

Stratigraphic Subdivision 2

AP-2

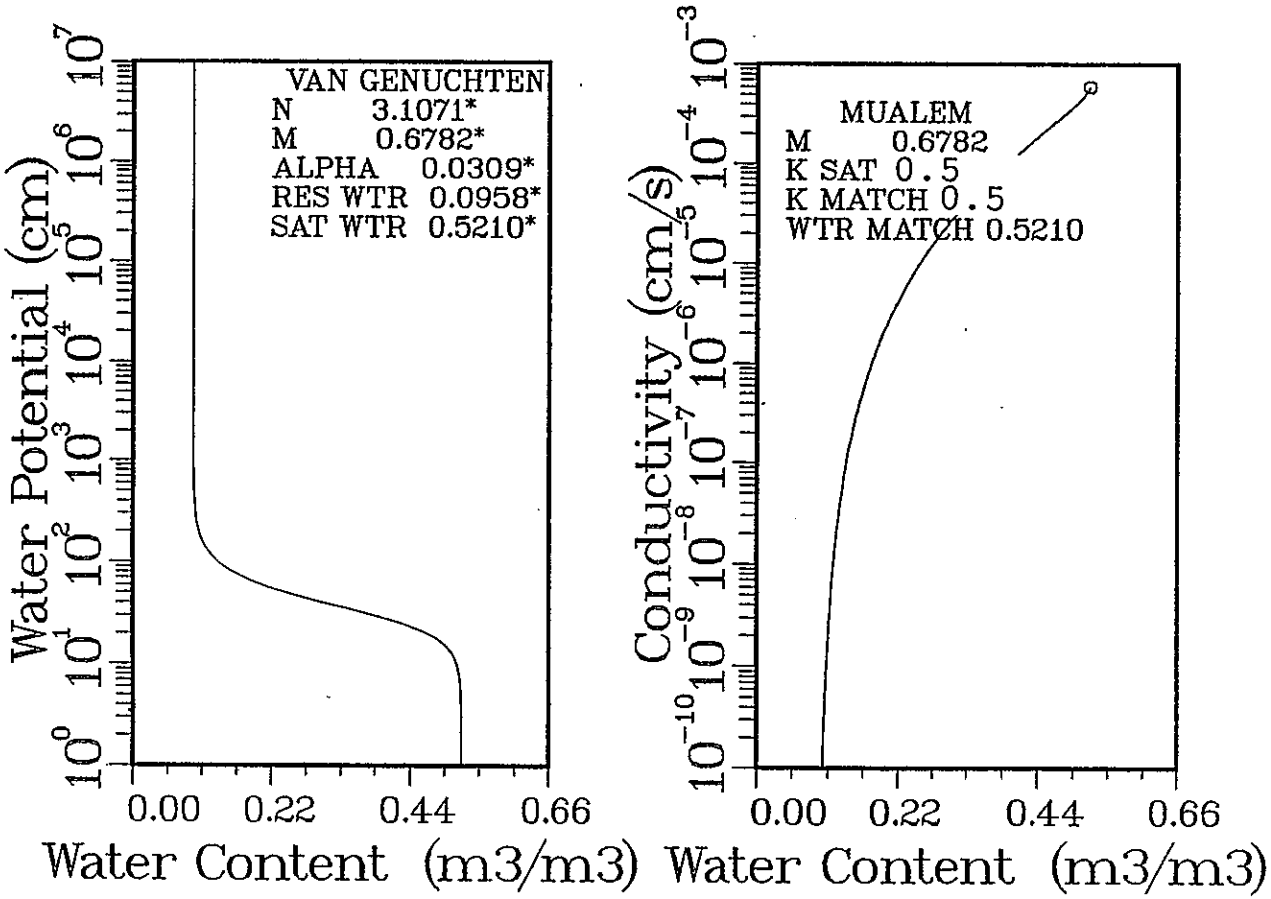

FIGURE 5.4. Moisture Retention Curves Identified for Stratigraphic Unit Two at the T Tank Farm

Stratigraphic Subdivision 3

AP-4G

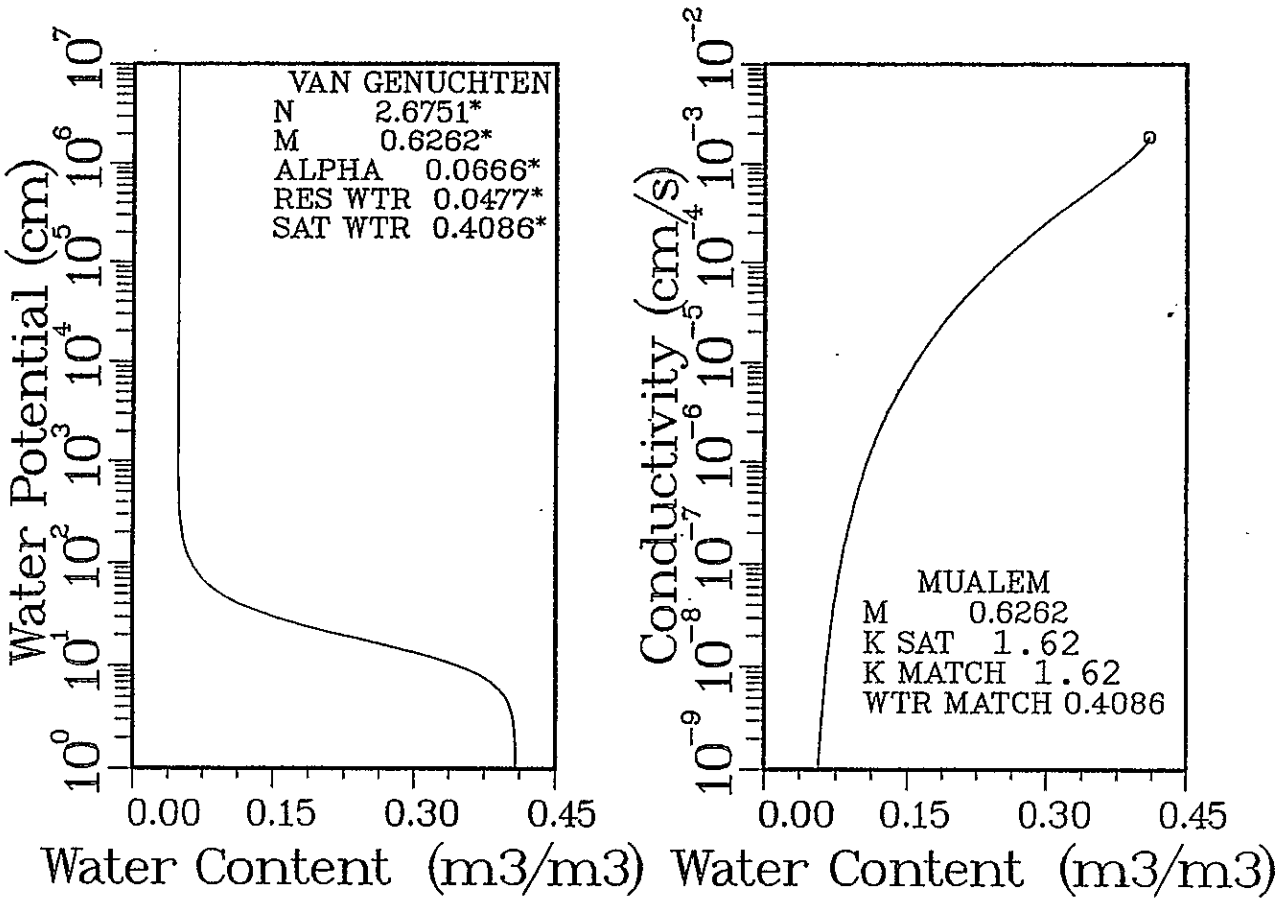

FIGURE 5.5. Moisture Retention Curves Identified for Stratigraphic Unit Three at the T Tank Farm

Stratigraphic Subdivision 4

AP-5

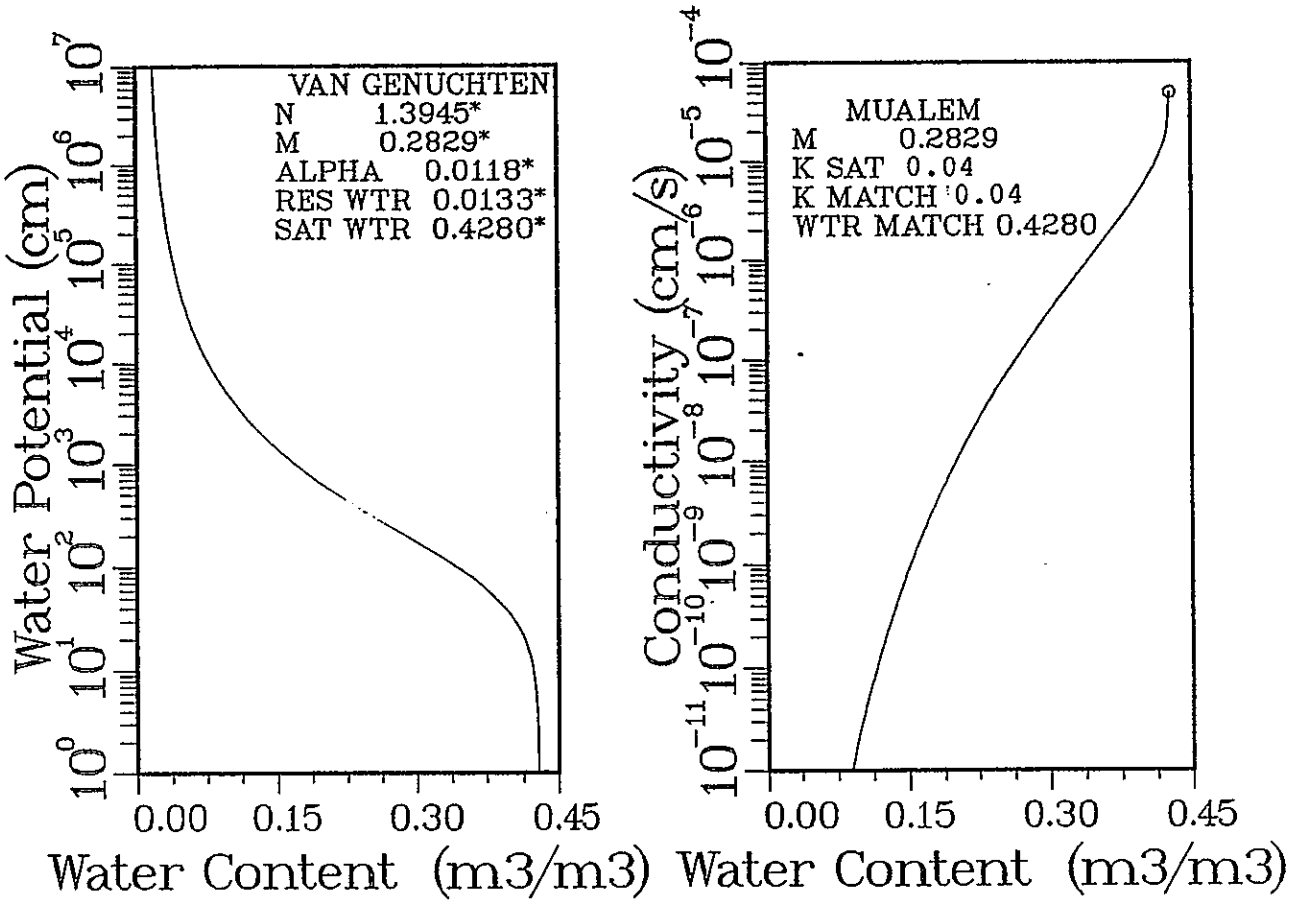

FIGURE 5.6. Moisture Retention Curves Identified for Stratigraphic Unit Four at the T Tank Farm

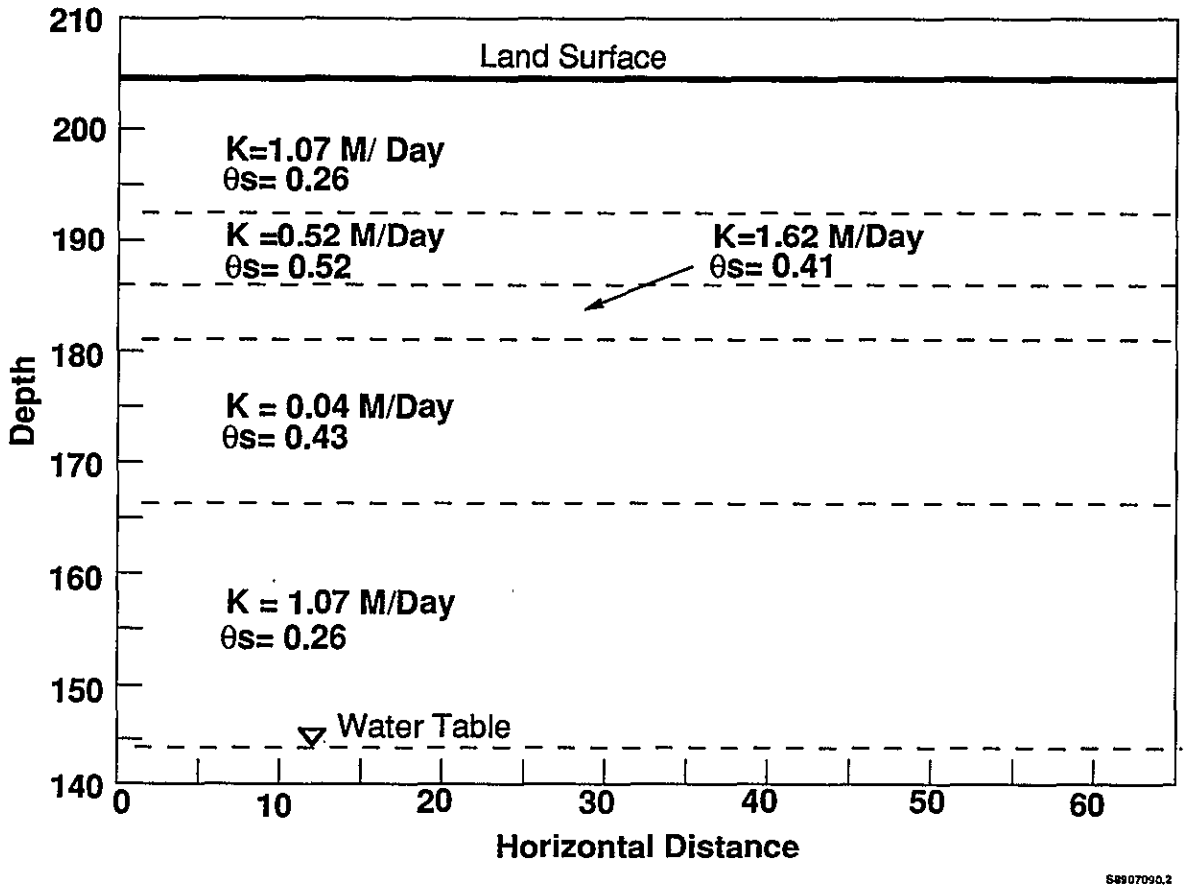

FIGURE 5.7. Hydraulic Coefficients for the Five Stratigraphic Units Identified at the T Tank Farm

5.5 SOURCE TERMS

The source terms for radionuclides are based on their concentrations in the supernate (Table 4.1). These concentrations were applied to the leak volume of 115,000 gallons for a duration of 52 days to generate a contaminant source term. The total inventory of about 2.7 x 10^{11} μCi of ^{106}Ru results in a source term of 5.1 x 10^{9} μCi/day during the 52-day leak. The corresponding liquid flux is about 8.4 m^3/day and is assumed to have the viscosity of water rather than supernate. The total inventory of ^{137}Cs of about 3.8 x 10^{10} μCi results in a source term of about 7.4 x 10^{8} μCi/day during the 52-day leak. The total liquid flux is assumed to remain constant for each constituent analyzed.

THIS PAGE INTENTIONALLY
LEFT BLANK

6.0 RESULTS OF SIMULATIONS

The 241-T-106 tank leak was simulated to portray contaminant plumes for ^{106}Ru and ^{137}Cs. The leak was assumed to continue for 52 days, after which the source of both liquid and contaminant was shut off. For the first series of simulations, the soil-moisture properties listed in a Hanford Site soil property data catalogue (Sewart et al. 1987) were used. The intent was to vary some of the input parameters in subsequent simulations as needed to better approximate the distribution of radionuclides in the soil column, as inferred from gamma spectrometry measurements in 1973 at a time approximately 100 days after the beginning of the leak. Using the calibrated properties, simulation continued through 1990 to estimate the current distribution of the plume.

6.1 SOIL MOISTURE MOVEMENT

The PORFLO-3 code provides output for soil moisture in terms of the degree of saturation for each time step. The two major sources of moisture in the simulations were infiltration from precipitation and the fluid introduced by the tank leak. The estimates of initial soil suction were based on unit gradient calculations for an average recharge flux of 0.05 m/yr, as discussed in Section 5.3. However, the initial soil suctions are only estimates and do not account for the additional flux adjacent to the tank that may result from the diversion of water around the domed top. The leak itself may be expected to produce a saturated slug of fluid that would move predominantly downward and dissipate by increasing the relative saturation of the underlying sediments. Consequently, the major features of interest with respect to the moisture movement and redistribution are the infiltration of meteoric water around the tank and the movement of the leaked fluid.

The redistribution of the leaked fluid is shown in Figures 6.1 through 6.6. Figure 6.1 shows the leak at a time of 150 days, or about 100 days after the free liquids in the tank were pumped out. The sediments immediately below the tank have begun to drain. The zone of higher saturation resulting from the leaked tank fluid is about 15 m below the base of the

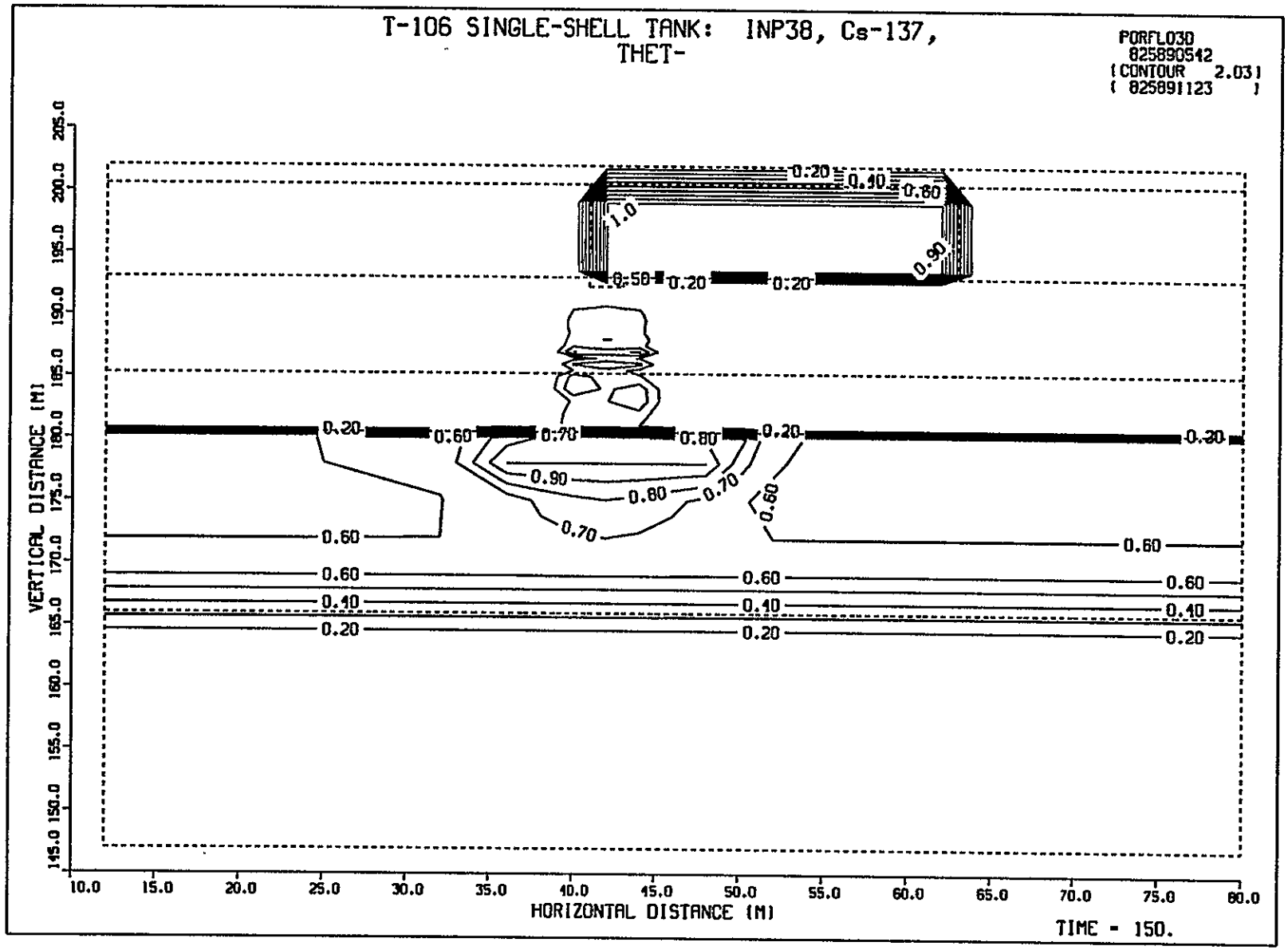

FIGURE 6.1. PORFLO-3 Simulation of Relative Saturation at 150 Days (Vertical Cross Section)

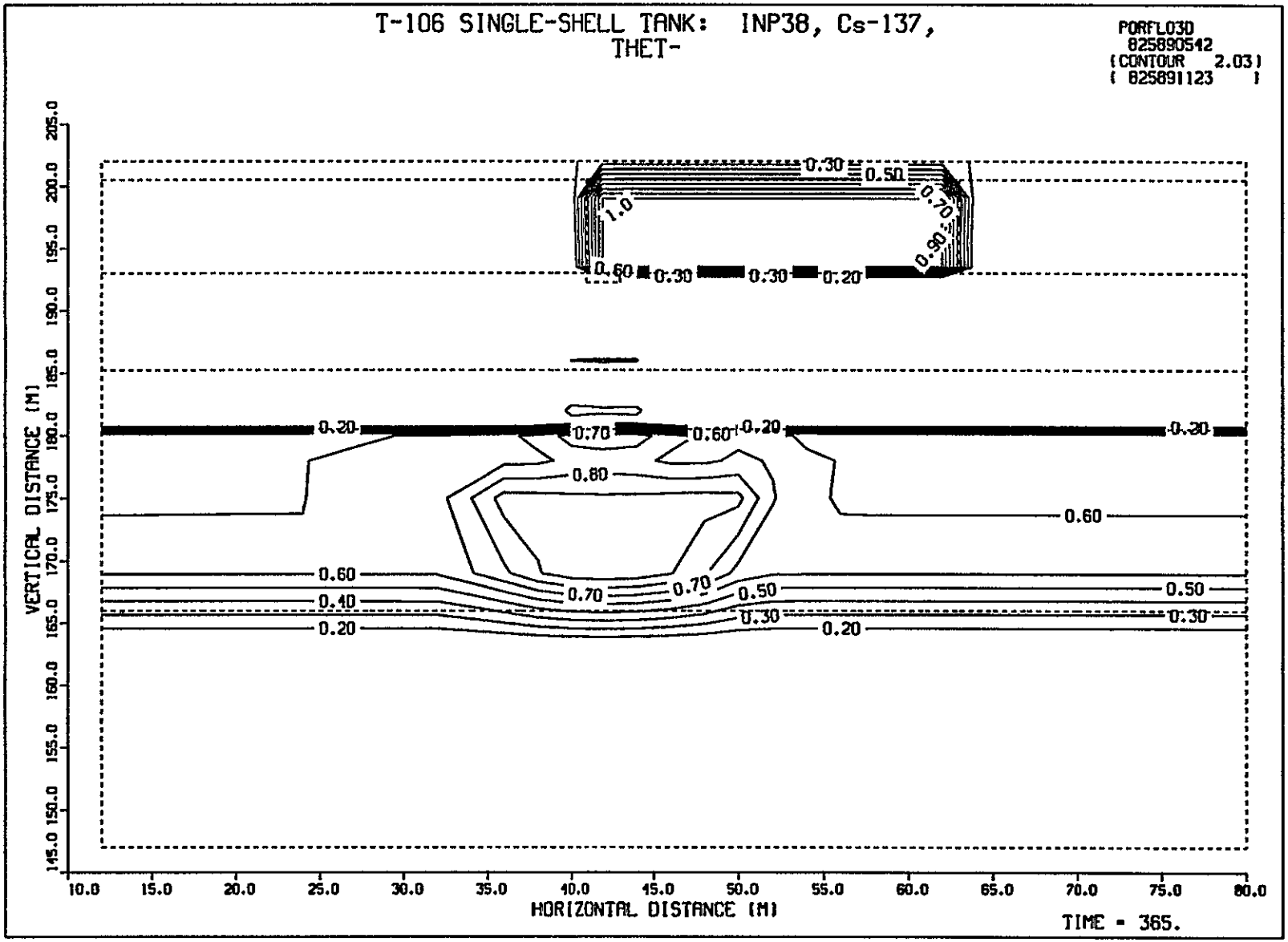

FIGURE 6.2. PORFLO-3 Simulation of Relative Saturation at 365 Days (Vertical Cross Section)

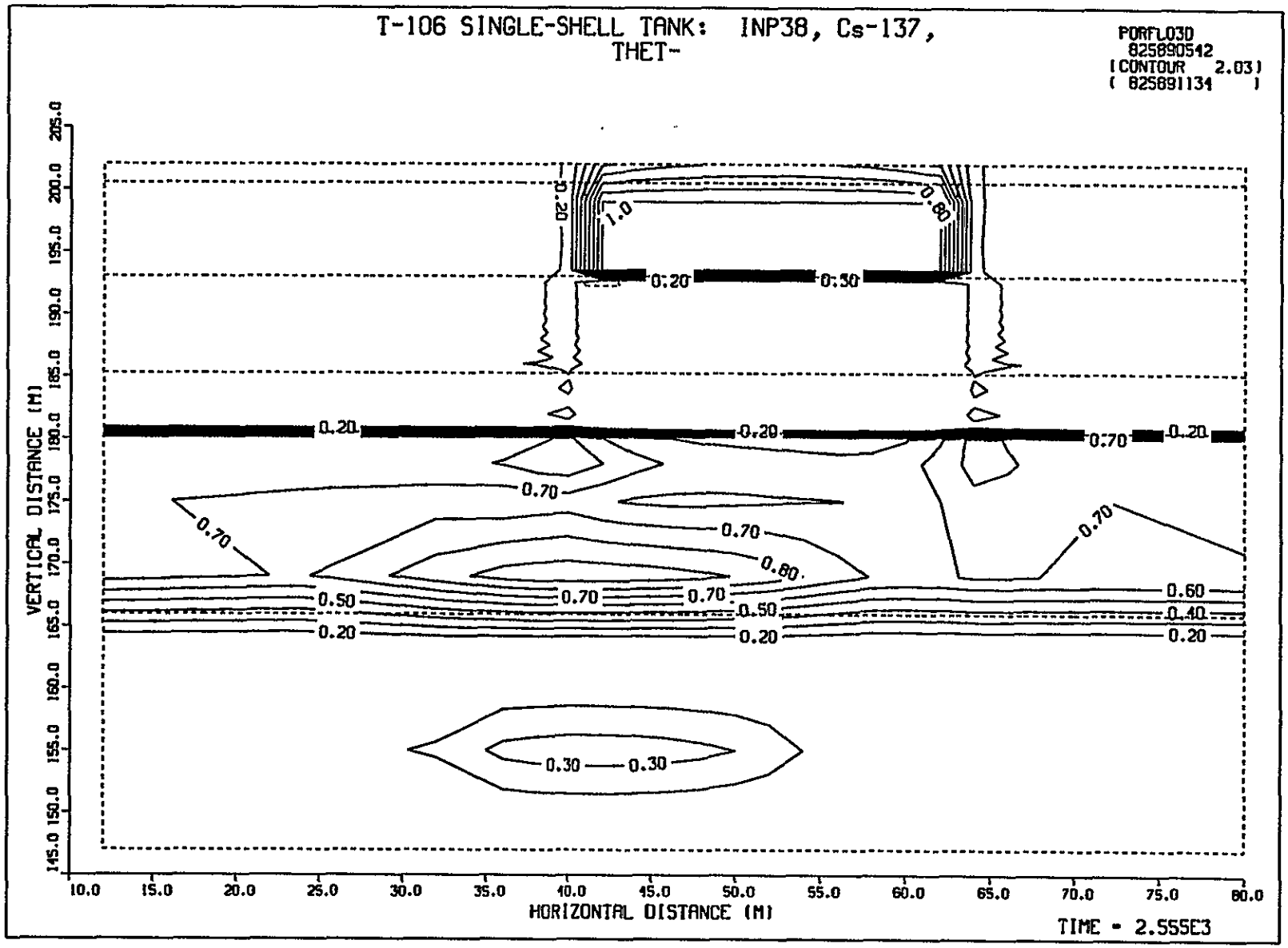

FIGURE 6.3. PORFLO-3 Simulation of Relative Saturation at 2,555 Days (Vertical Cross Section)

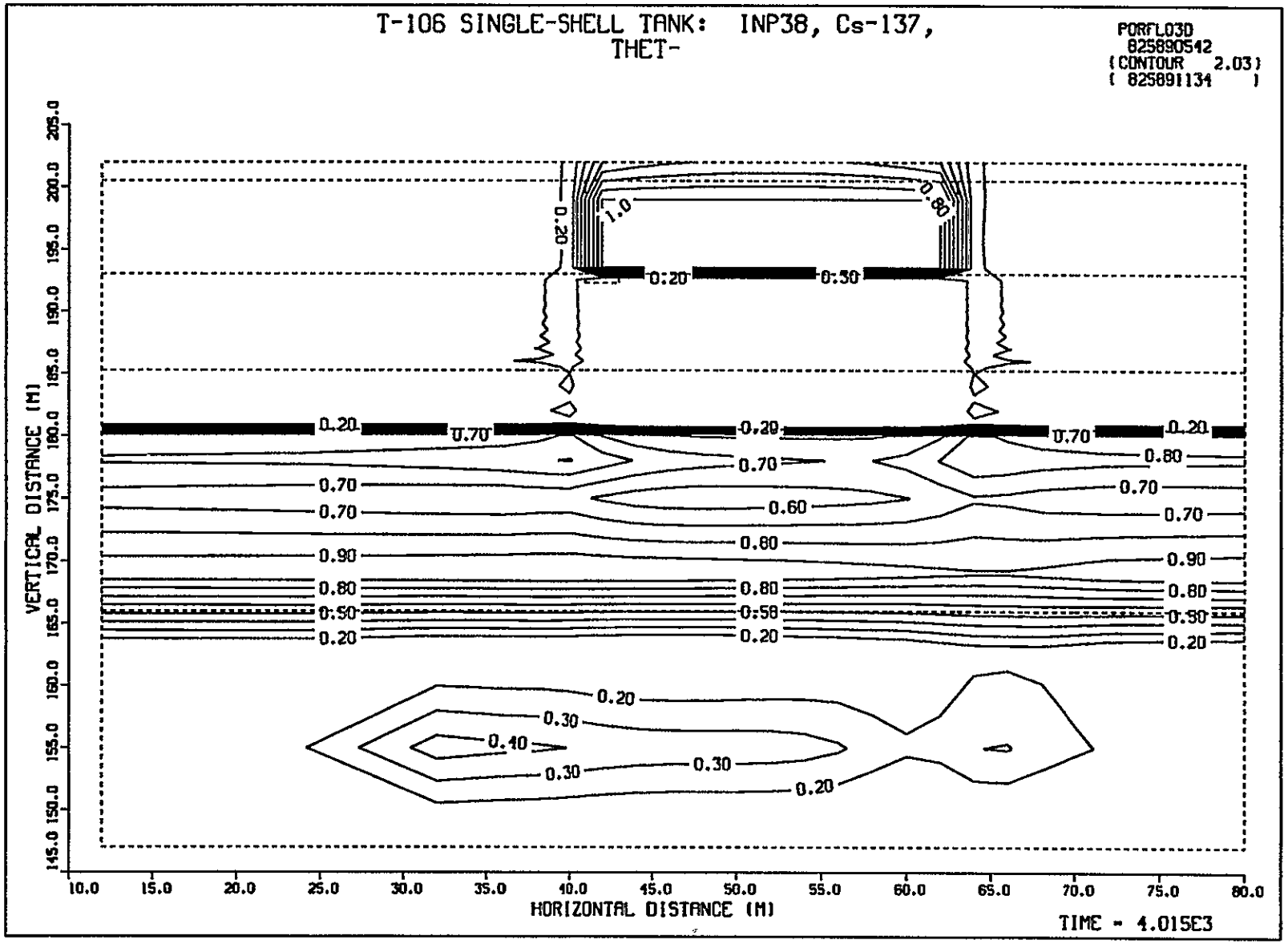

FIGURE 6.4. PORFLO-3 Simulation of Relative Saturation at 4,015 Days (Vertical Cross Section)

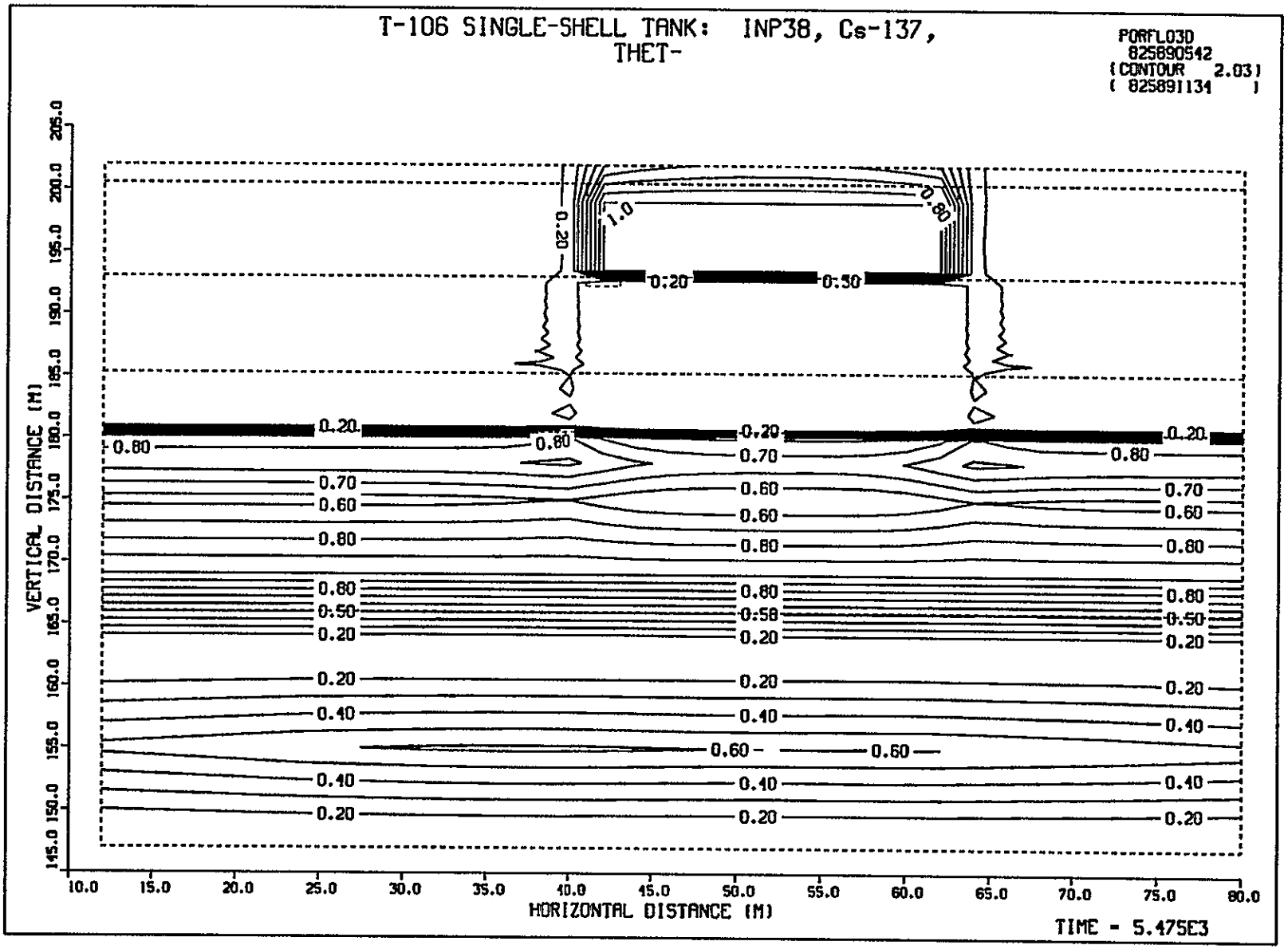

FIGURE 6.5. PORFLO-3 Simulation of Relative Saturation at 5,475 Days (Vertical Cross Section)

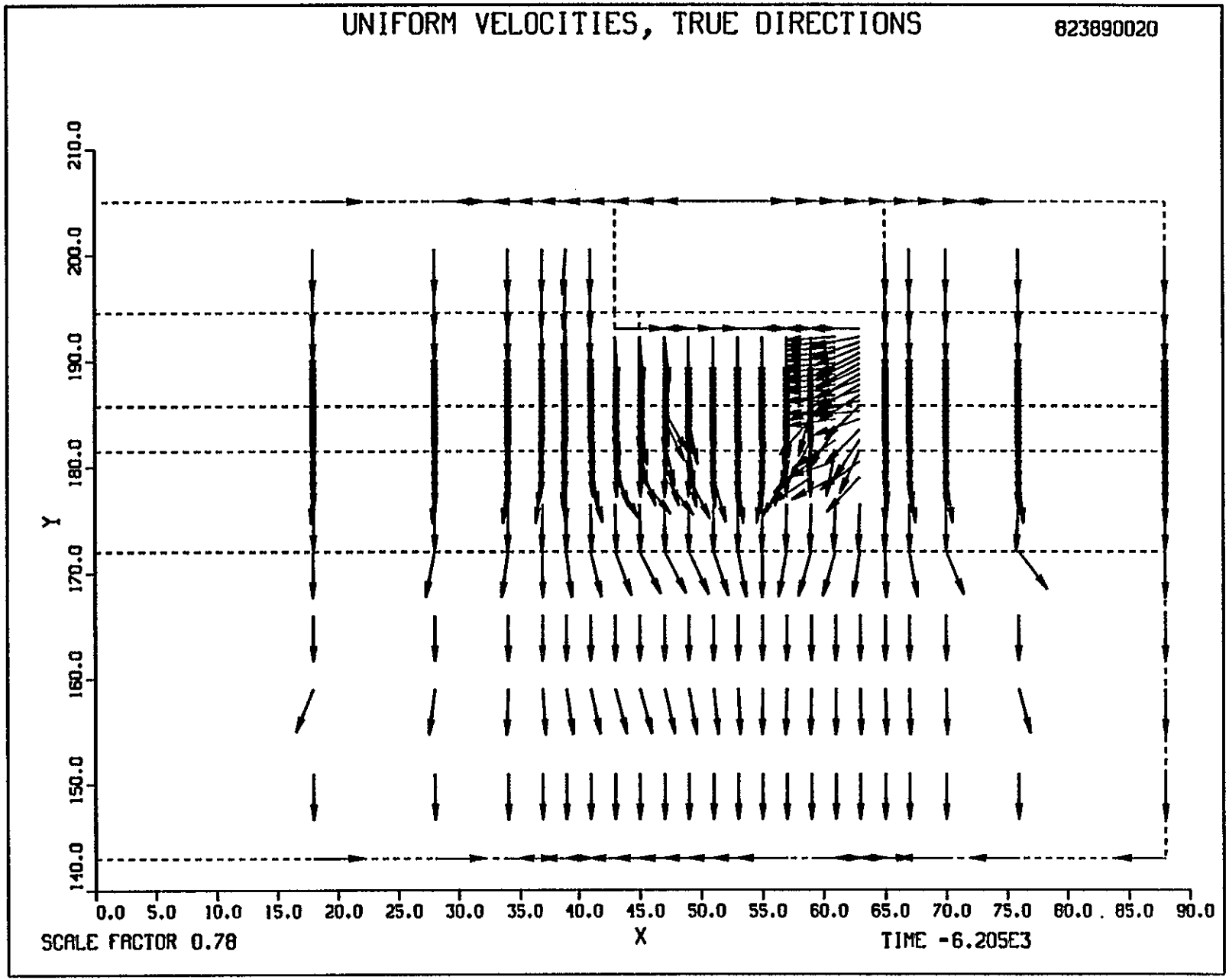

FIGURE 6.6. PORFLO-3 Simulation of Water Velocities at 100 Days (Vertical Cross Section)

tank in the top of stratigraphic unit 4 (see Figure 3.2). Unit 4 has a lower porosity than unit 3 and a much lower saturated hydraulic conductivity; these factors can be expected to inhibit spread of the fluid. The increase in saturation near the top of the finer-grained sediments in unit 4 appears to be a reasonable result. Isaacson (1982) reported saturated or near-saturated conditions in T Tank Farm dry wells at approximately this depth.

At the later times shown in Figures 6.2 through 6.5, the slug of fluid continues to drain and dissipate. Also evident at later times is an increase in saturation from infiltrating water diverted along the wall of the tank. Velocity vectors showing the direction of water movement in the same cross section (Figure 6.6) indicate that water is moving laterally across the dome of the tank, down the tank wall, and perhaps refracting slightly as it enters the sediments below the tank. These results suggest that the initial conditions based on a 0.05 m/yr rate of infiltration of meteoric water are not a good assumption for the vicinity of the tank. Diversion of water around the tank is likely to elevate soil moisture conditions in the vicinity of the tank. Given a surface area of about 410 m^2 for the top of the tank, the volume of water that would be diverted during the 30 years prior to the leak would be about 1.5 leak volumes. Consequently, the resulting increase in soil moisture would tend to facilitate the movement of fluid leaking from the tank. A better initial condition would be to approximate the steady-state moisture flux around the tank prior to simulating the leak.

6.2 RUTHENIUM-106 PLUME

The results for ^{106}Ru, using the soil catalogue properties, are shown in vertical and horizontal cross section in Figures 6.7 and 6.8. These results indicate a migration of the 1-μCi/L isopleth for ^{106}Ru to a depth of about 40 m below the tank by 150 days after the beginning of the leak. The magnitude of this simulated migration is about twice that observed in the dry wells adjacent to the tank, as reported by Routson et al. (1979). Although discrepancies in the plume measurements may result from the absence of measurements under the tank and conversion of gamma counts to concentrations, for the purpose of this analysis the 1973 data on the extent of the plume

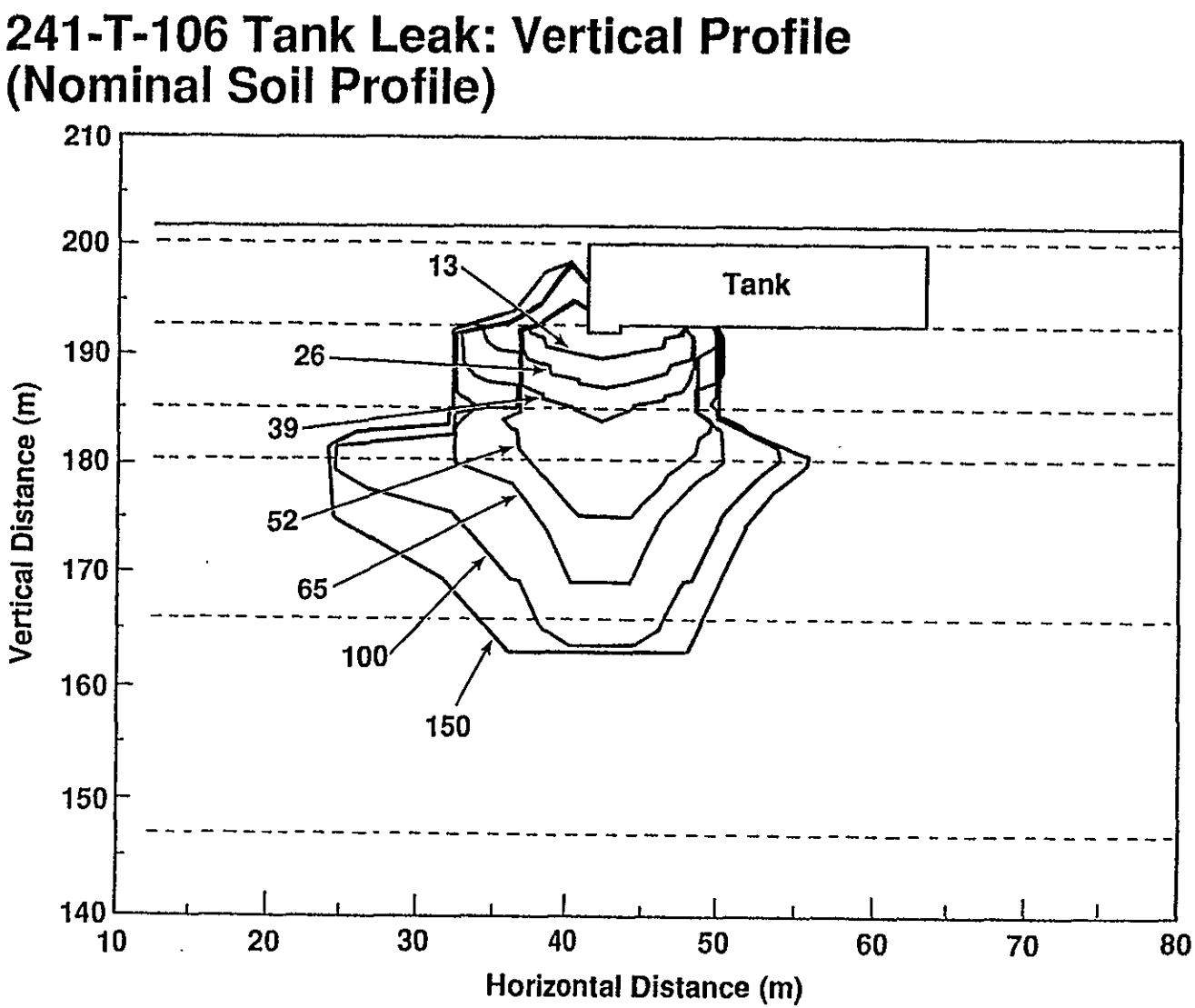

FIGURE 6.7. PORFLO-3 Simulation of the Vertical Extent of the ^{106}Ru 1-μCi/L Isopleth Using Data from Field Measurements

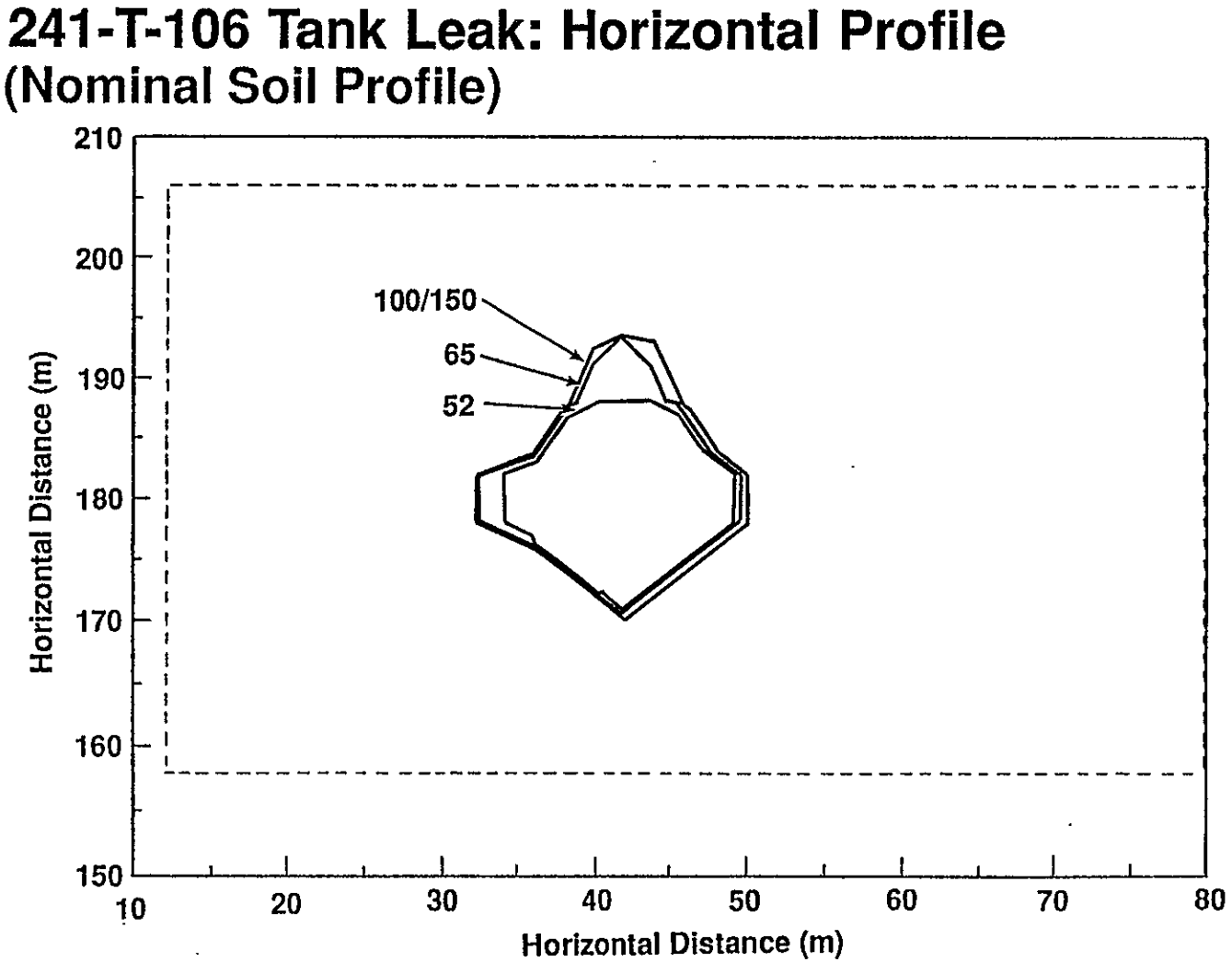

FIGURE 6.8. PORFLO-3 Simulation of the Horizontal Extent of the ^{106}Ru 1-μCi/L Isopleth Using Data from Field Measurements

are assumed to be correct. The rate of plume migration in the vertical direction that can be inferred from the measured extent of the plume is, therefore, slower than that indicated by the simulation results. The horizontal cross section shown in Figure 6.8 is about 5 m below the base of the tank and indicates a 1-μCi/L isopleth for ^{106}Ru of about 30 m in diameter. This dimension compares favorably with a diameter of 30 to 40 m of the measured horizontal spread reported by Routson et al. (1979).

Using the simulation results shown in Figures 6.7 and 6.8, several adjustments in the input data were made to better match the measured vertical extent of the ^{106}Ru plume. First, the vertical hydraulic conductivity (K_z) was reduced by a factor of two. The lower value of vertical hydraulic conductivity can be justified because the viscosity of the supernate liquid is higher than that of water. In addition, a factor of two is within the range of uncertainty that would be expected to result from the hydraulic anisotropy of the sediments.

Vertical and horizontal cross sections of the ^{106}Ru plume simulation using the adjusted Kd are shown in Figures 6.9 through 6.11 for times within 1 year of the leak. The 1-μCi/L isopleth for ^{106}Ru was located approximately 20 m below the base of the tank 150 days after the leak; this is in agreement with measurements reported by ARHCO (1973) and Routson et al. (1979). The diameter of the horizontal extent of the plume remains at approximately 30 m, which also compares favorably with the measured extent. Consequently, the simulation appears to be reasonably well calibrated to the 1973 data.

Simulations were subsequently made for the time period through 1990 to estimate the current extent of the plume. Figures 6.12 and 6.13 show the vertical and horizontal extent of the plume for several years up to 1990. The simulations show that the 1-μCi/L isopleth for ^{106}Ru has migrated through much of the soil column above the water table by the early 1980s. Radioactive decay then appears to reduce the extent of the plume through the remainder of the time. However, the simulation predicts that the 1-μCi/L isopleth for ^{106}Ru will encompass a relatively large part of the soil column. This result appears to be a consequence of the large initial inventory of

241-T-106 Tank Leak: Vertical Profile

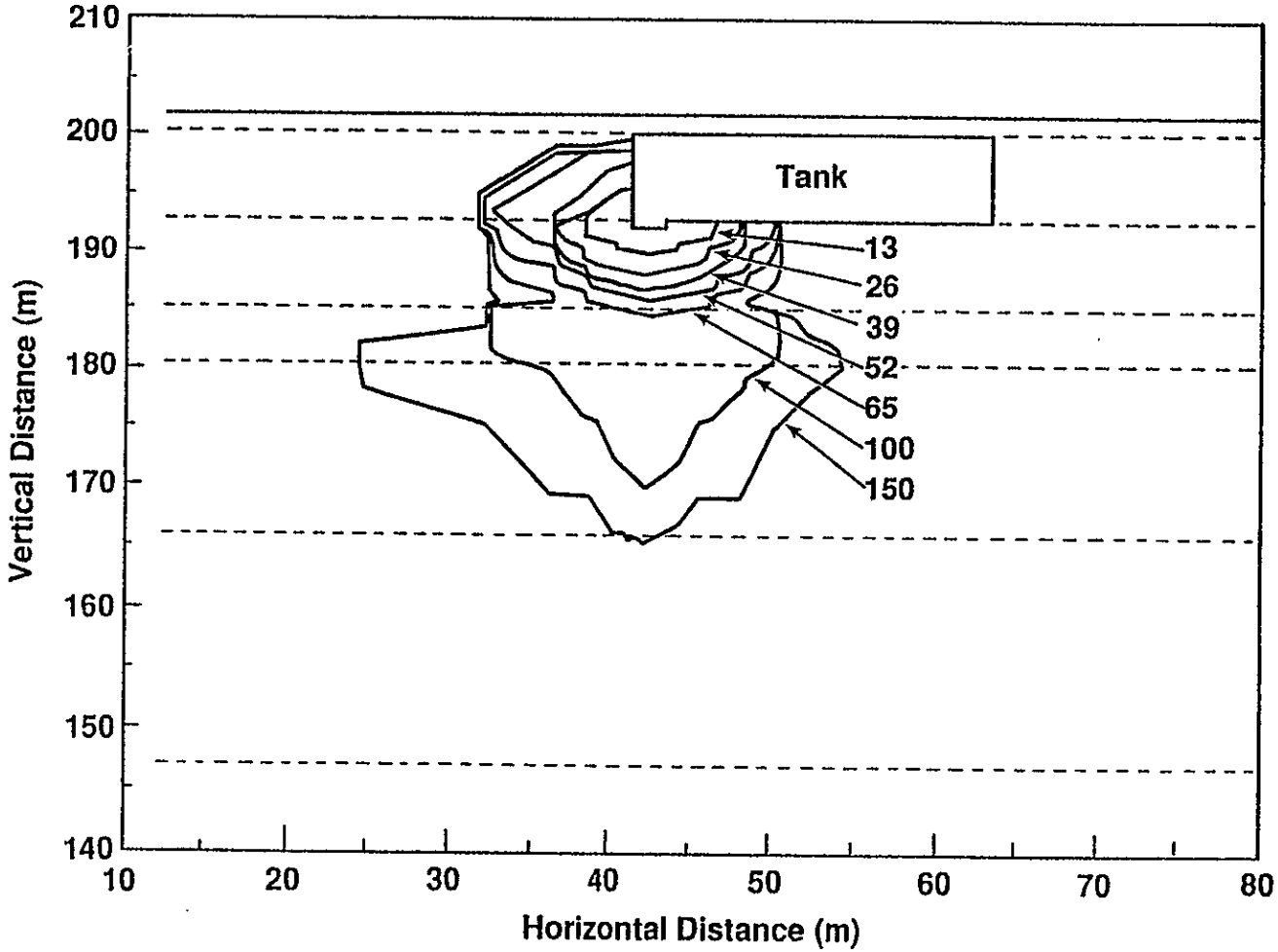

FIGURE 6.9. PORFLO-3 Simulation of the Vertical Extent of the ^{106}Ru 1-μCi/L Isopleth With Adjusted Vertical Hydraulic Conductivity at Early Simulation Times

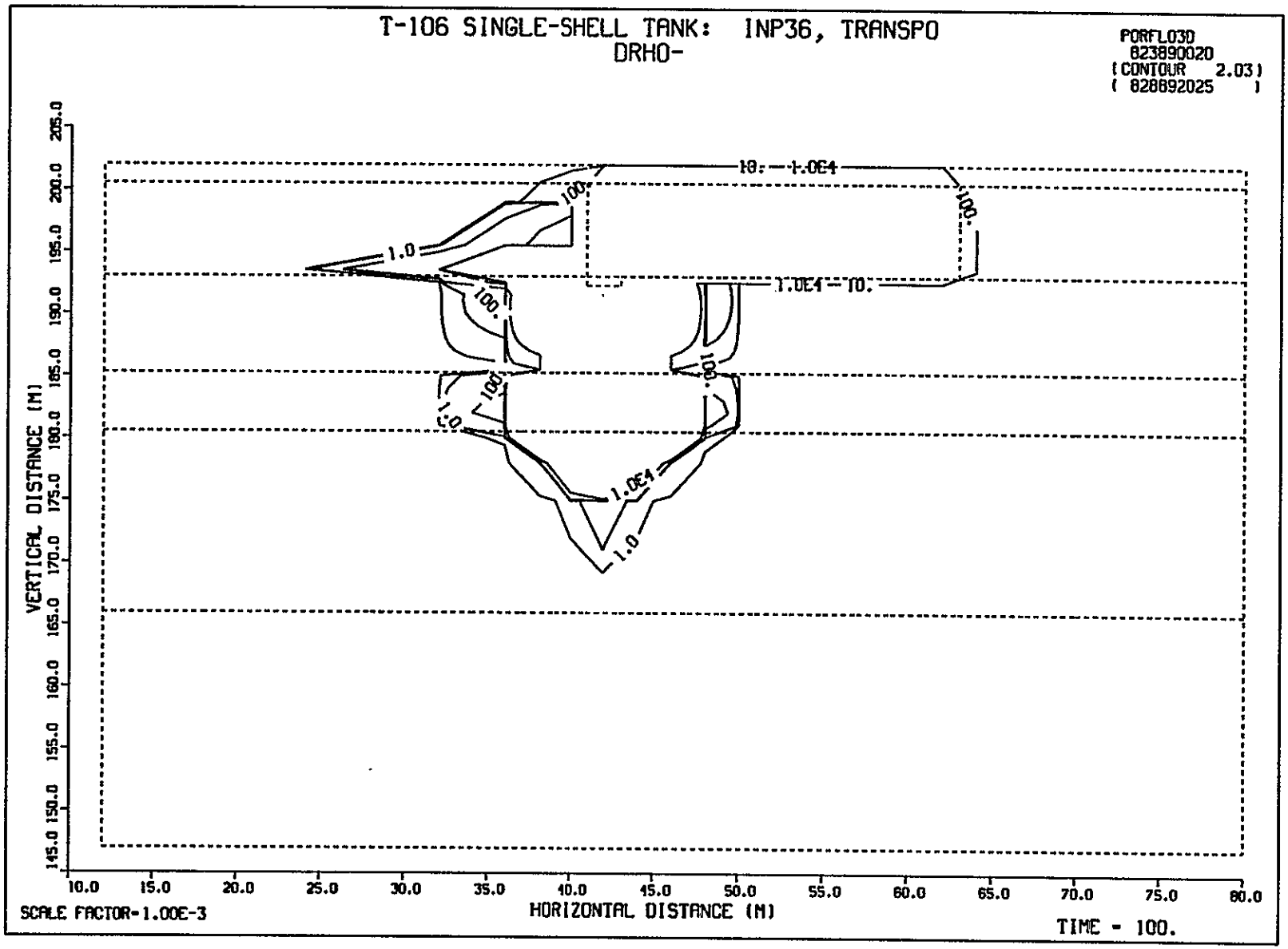

FIGURE 6.10. PORFLO-3 Simulation of the Vertical Extent of the ^{106}Ru After 100 Days With Adjusted Vertical Hydraulic Conductivity

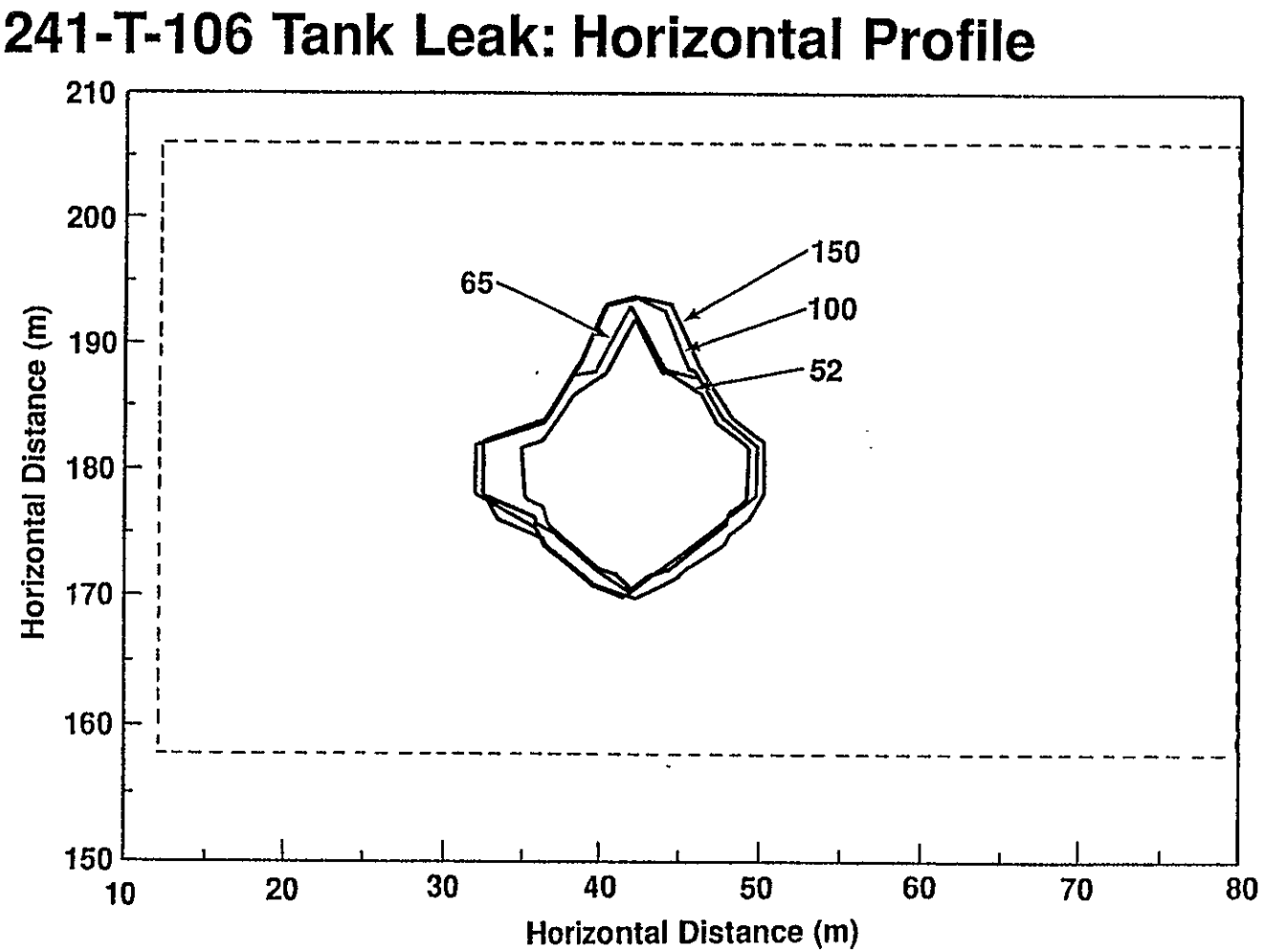

FIGURE 6.11. PORFLO-3 Simulation of the Horizontal Extent of the ^{106}Ru 1-μCi/L Isopleth With Adjusted Vertical Hydraulic Conductivity at Early Simulation Times

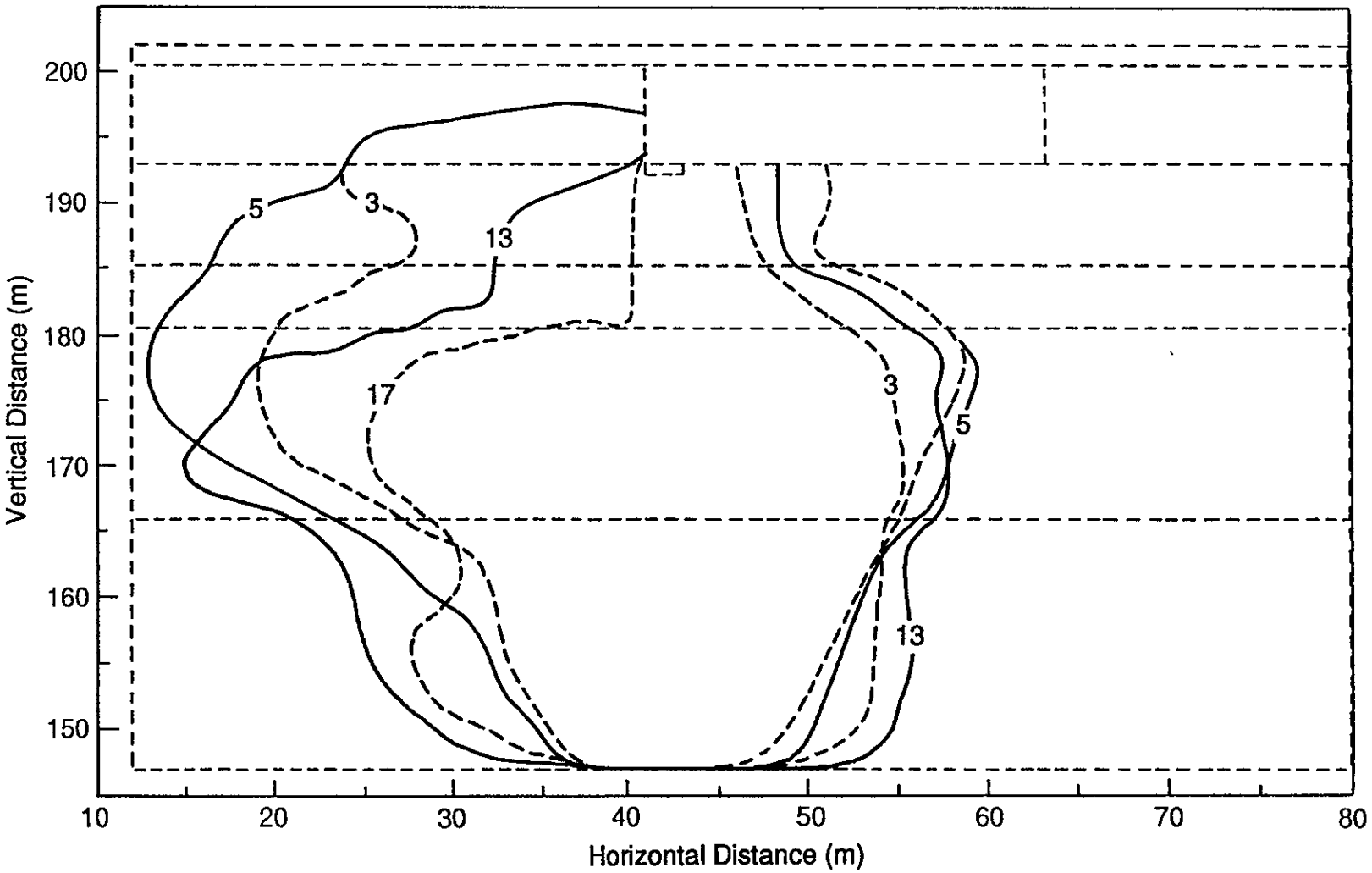

FIGURE 6.12. PORFLO-3 Simulation of the Vertical Extent of the ^{106}Ru 1-μCi/L Isopleth With Adjusted Vertical Hydraulic Conductivity at Late Simulation Times

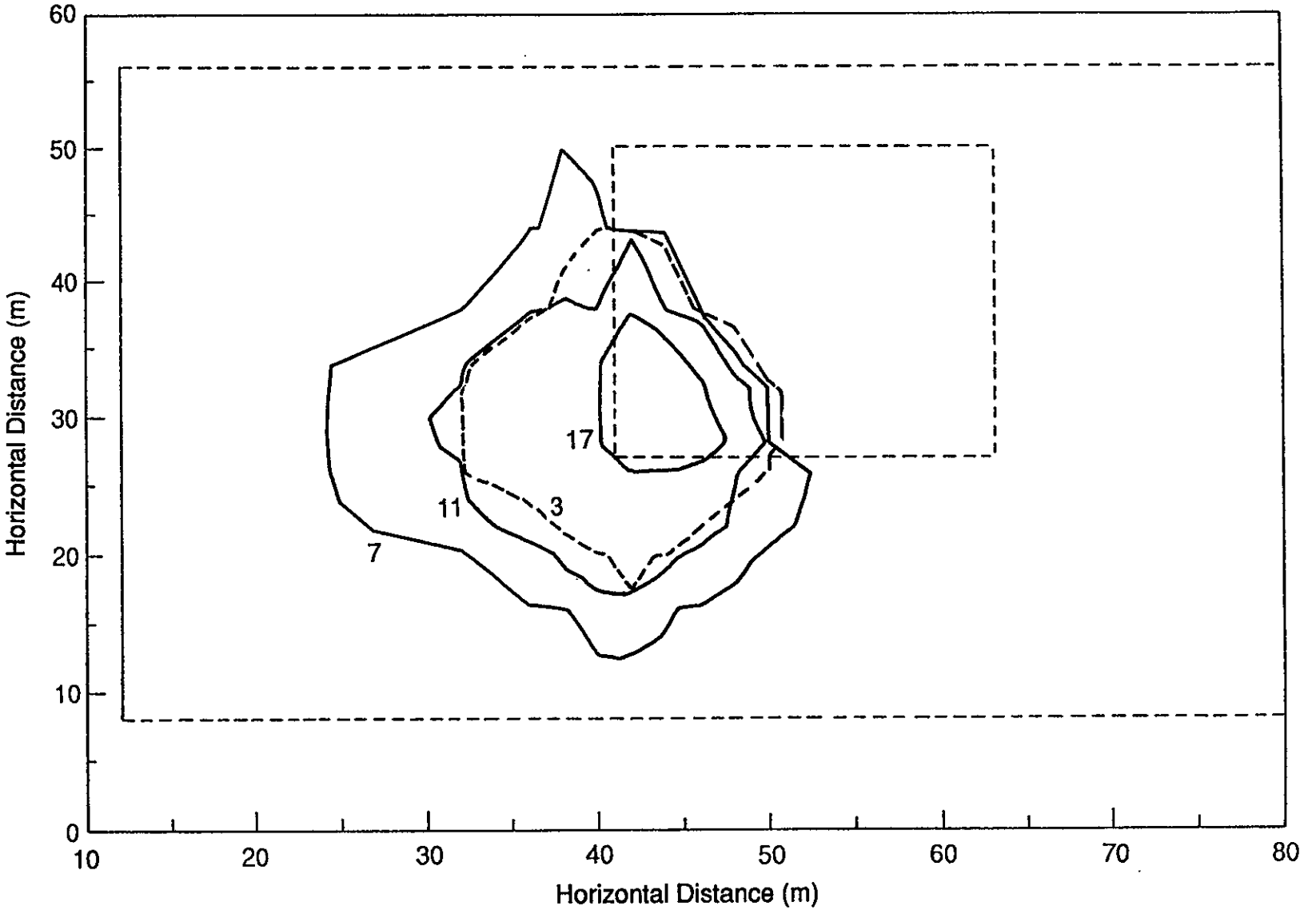

FIGURE 6.13. PORFLO-3 Simulation of the Horizontal Extent of ^{106}Ru 1-μCi/L Isopleth With Adjusted Vertical Hydraulic Conductivity at Late Simulation Times

ruthenium. Radioactive decay of ^{106}Ru appears to only moderately affect reduction of the simulation plume by 1990, as defined by the 1-μCi/L isopleth for ^{106}Ru.

The degree to which ^{106}Ru is adsorbed by Hanford Site soils is uncertain. Ruthenium-106 tends to act as a cation at a pH of less than about 5, and as an anion at a pH greater than 5 (Ames and Rai 1978). Because Hanford Site soils tend to be neutral to slightly basic and the supernate waste solution in the T-106 Tank had a pH of about 12, cation exchange is probably not a major factor in sorption of ^{106}Ru. Coles and Ramspott (1982) and Ames and Rai (1978) both report that ^{106}Ru moves approximately with the water through soil columns of varying composition, as was the case in the initial set of simulations. However, work by Murthy et al. (1983) indicated that a retardation factor (less than 5) may be associated with ^{106}Ru. Therefore, a second set of simulations was made incorporating a small retardation factor (partition coefficient of 0.5 mL/g) to account for adsorption of ^{106}Ru. A Kd of 0.5 mL/g was used, resulting in retardations ranging from about 2.5 to 4 in response to the different porosities of each stratigraphic unit. All other conditions used in the initial set of simulations were held constant.

The results of this simulation are shown in Figures 6.14 through 6.16 for both vertical and horizontal sections through the plume. At 150 days after the beginning of the leak, the plume is about 25 m below the base of the tank. The horizontal diameter of the 1-μCi/L isopleth for ^{106}Ru is about 10 m at a depth of about 10 m below the tank. The vertical extent of the plume is similar to that reported by Routson et al. (1979), but the horizontal extent is somewhat smaller.

The simulation isopleths for times of more than 1 year after the leak differ significantly from the simulations that use the unreduced K_z. The latter show the 1-μCi/L isopleth for ^{106}Ru migrating through much of the soil column above the water table by the early 1980s, but the plume then appears to recede rapidly with the passage of additional time. One explanation could be that retardation causes the concentration gradient between the centroid of the plume and the 1-μCi/L isopleth for ^{106}Ru to be

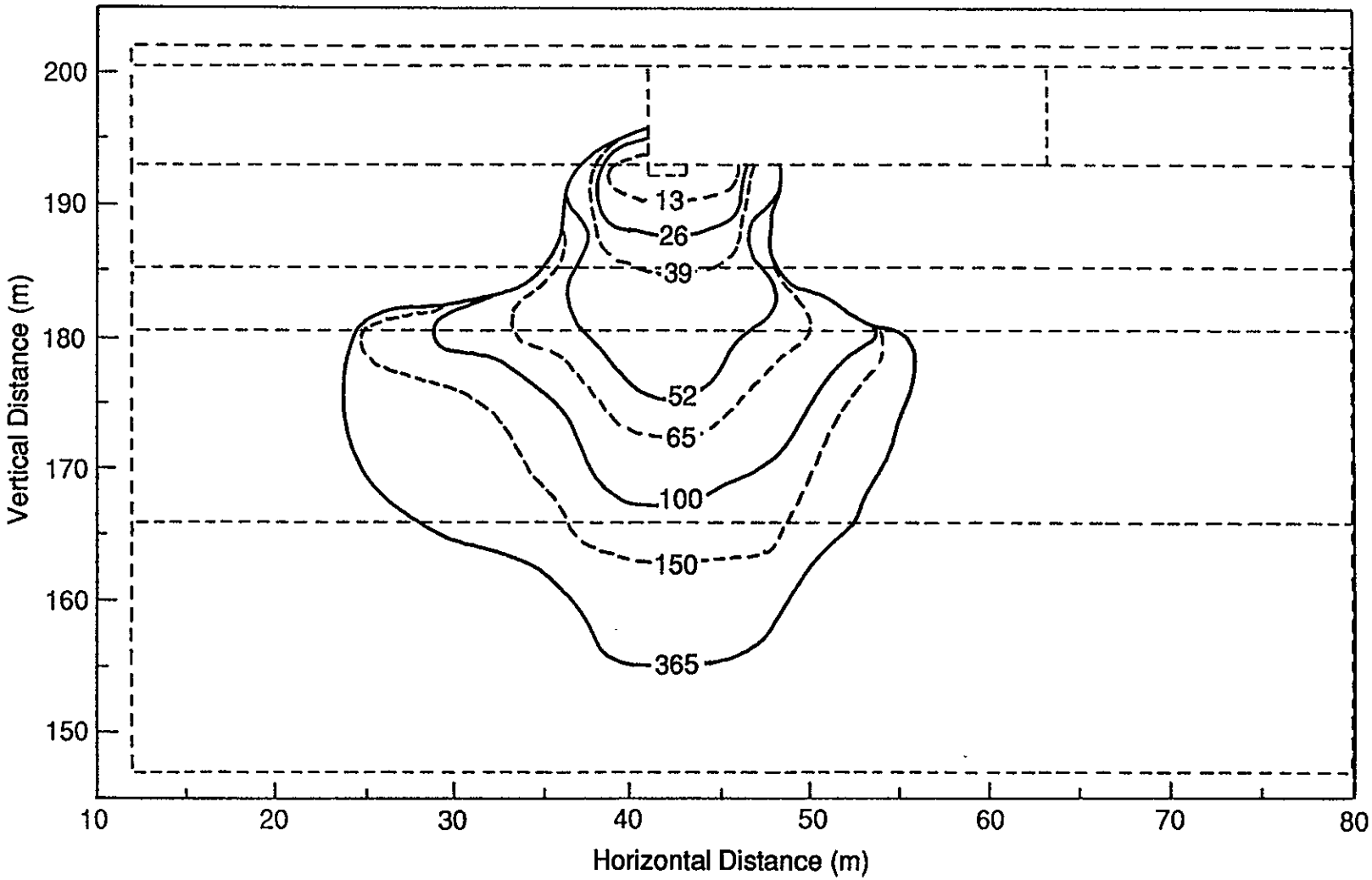

FIGURE 6.14. PORFLO-3 Simulation of the Vertical Extent of the ^{106}Ru 1-μCi/L Isopleth for Hydraulically Isotropic Stratigraphic Units With a Distribution Coefficient of 0.5 mL/g at Early Simulation Times

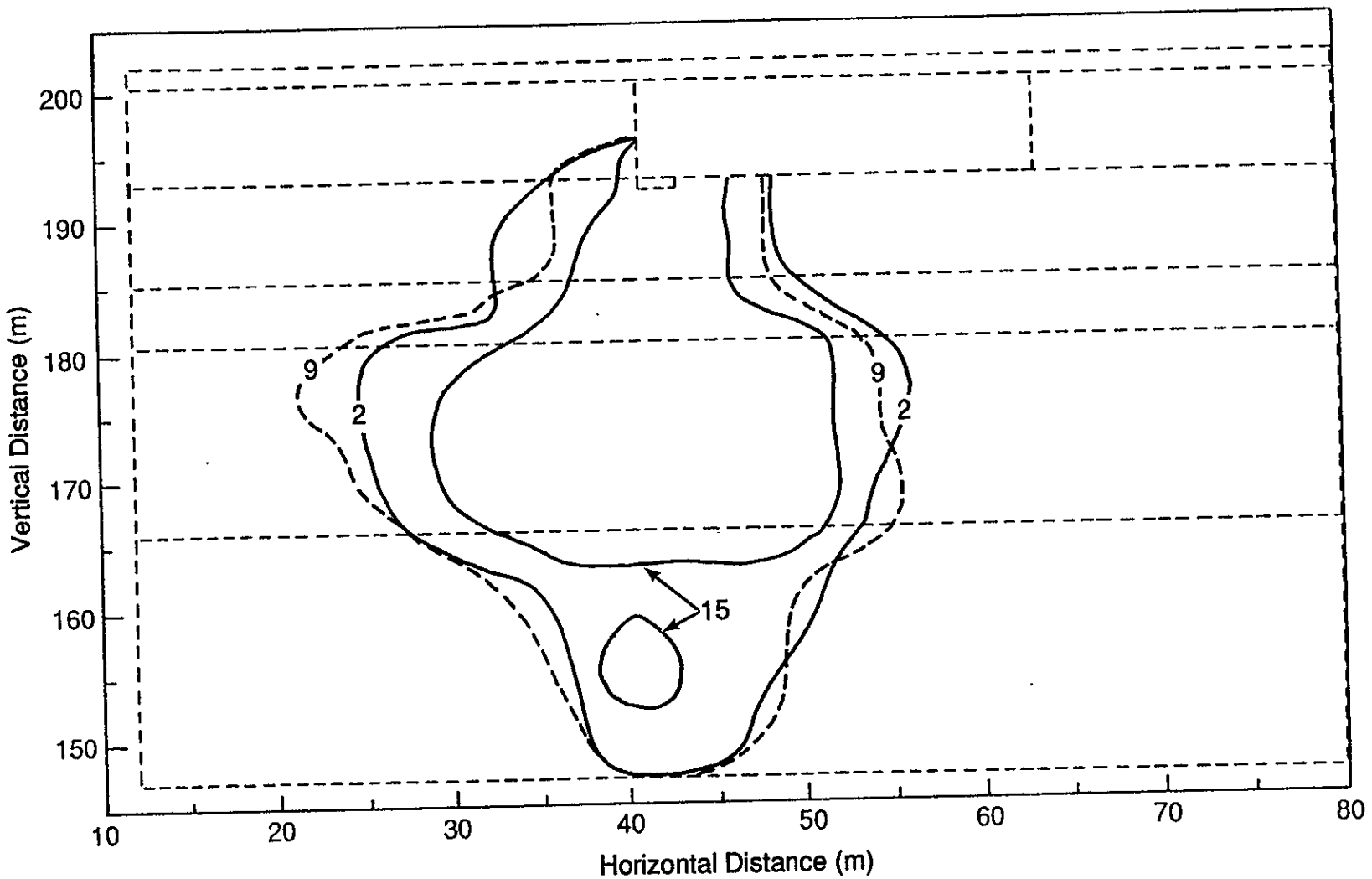

FIGURE 6.15. PORFLO-3 Simulation of the Vertical Extent of the ^{106}Ru 1-μCi/L Isopleth for Hydraulically Isotropic Stratigraphic Units With a Distribution Coefficient of 0.5 mL/g at Late Simulation Times

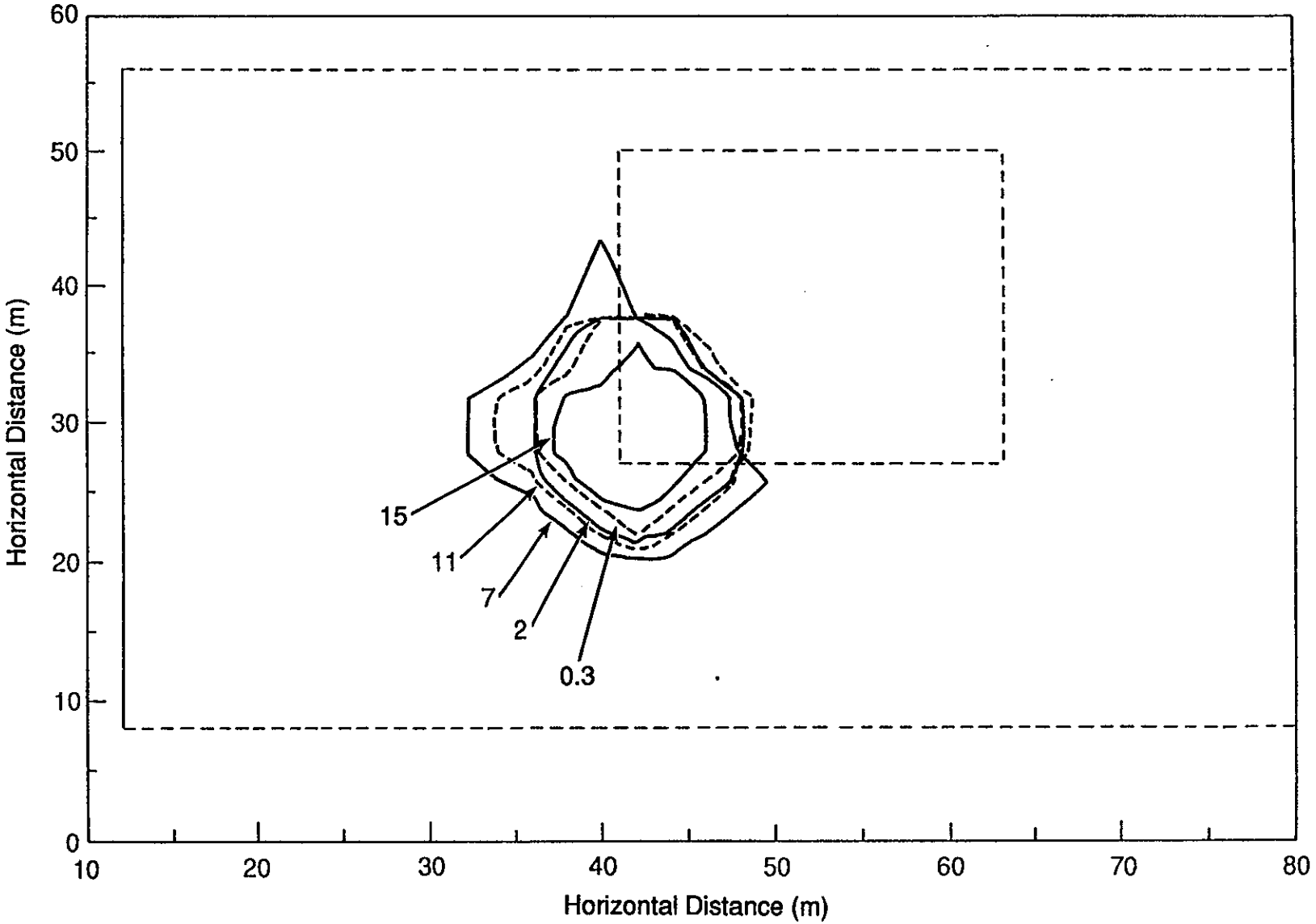

FIGURE 6.16. PORFLO-3 Simulation of the Horizontal Extent of the ^{106}Ru 1-μCi/L Isopleth for Hydraulically Isotropic Stratigraphic Units With a Distribution Coefficient of 0.5 mL/g

parabolic, thus resulting in effects of radioactive decay on the 1-μCi/L isopleth that are larger because of the smaller slope of the concentration gradient near the 1-μCi/L isopleth.

The plume resulting from the simulation using a retardation coefficient appears to be more compact at early simulation times than the plume resulting from the simulation using a reduced vertical hydraulic conductivity. In other words, the plume that incorporates retardation appears to have a smaller surface-area-to-volume ratio than that resulting from a reduced K_z. This result appears reasonable; a reduction in K_z would tend to reduce the vertical migration of the plume and force it to spread laterally in the x and y directions, resulting in a larger surface-area-to-volume ratio in three dimensions. The retardation factor, however, would tend to inhibit movement in all three directions. For a grid cell in the interior of a given stratigraphic unit, the retardation factor should dampen contaminant transport equally in any direction for a unit flux of contaminant. However, there will be small differences in retardation for grid cells located along unit boundaries because of the slightly different retardation coefficients for each stratigraphic unit.

In general, the simulations for ^{106}Ru indicate that the 210-AP tank farm soil properties used to represent the soil column in the vicinity of the 241-T-106 tank are adequate for approximating the plume in three dimensions with relatively little adjustment. It will likely be possible to more closely simulate the actual ^{106}Ru leak with the PORFLO-3 code when site-specific field data become available.

6.3 CESIUM-137 PLUME

A simulation was made for the ^{137}Cs plume using input parameters equivalent to those used for ^{106}Ru. The same hydraulic properties were used. Cesium-137 has a half-life of about 1.1×10^4 days (30 years) and is much less mobile in Hanford Site soils than ^{106}Ru. For the simulation, a Kd of 1.0×10^{-4} m^3/g (100.0 mL/g) was used, resulting in retardations ranging between about 320 and 640.

Results of the initial simulation for ^{137}Cs are shown for vertical and horizontal cross sections in Figures 6.17 and 6.18. The 1-μCi/L isopleth for ^{137}Cs has migrated to a depth of only several meters below the tank at

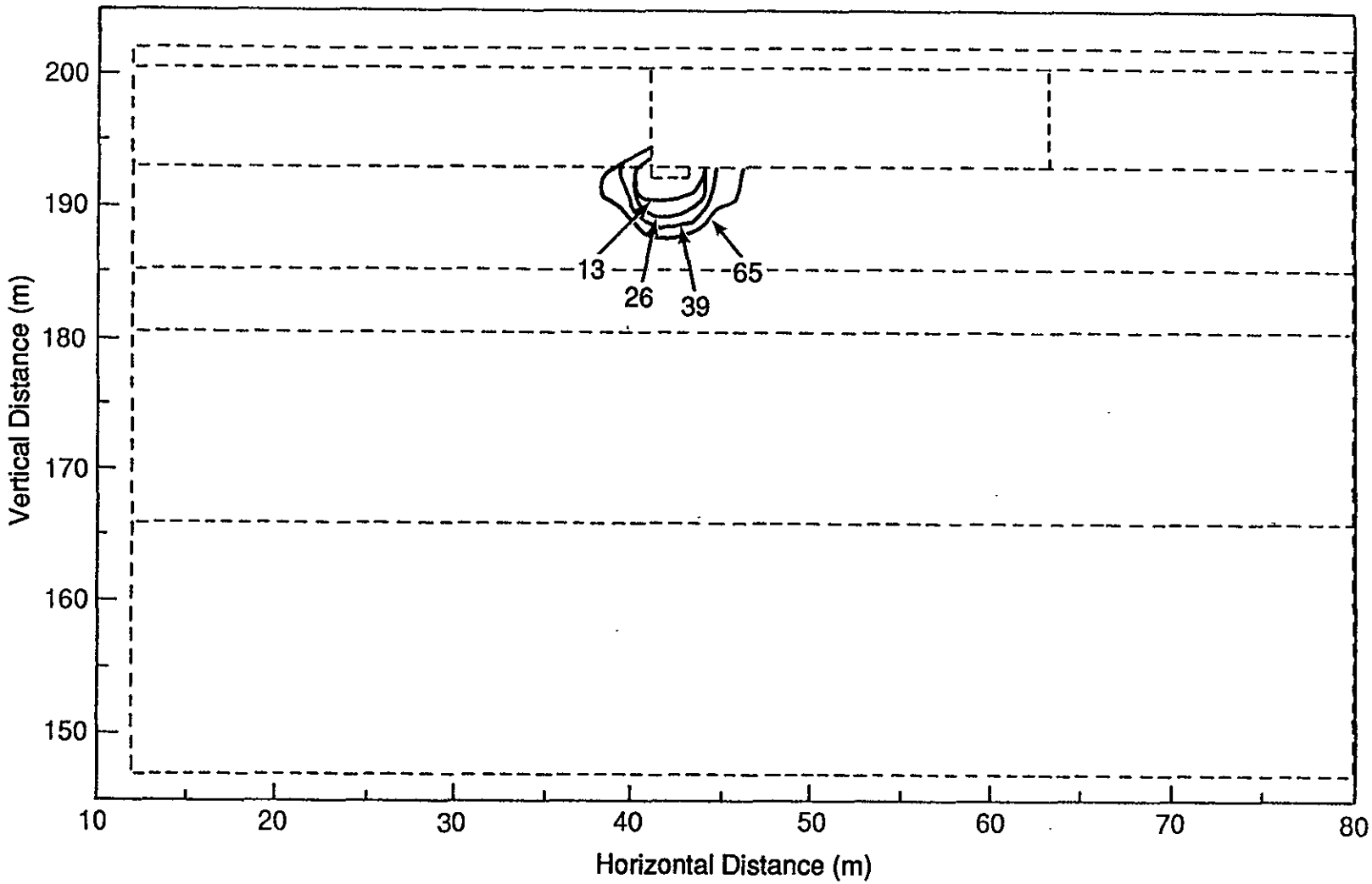

FIGURE 6.17. PORFLO-3 Simulation of the Vertical Extent of the ^{137}Cs 1-μCi/L Isopleth Using Data from Field Measurements

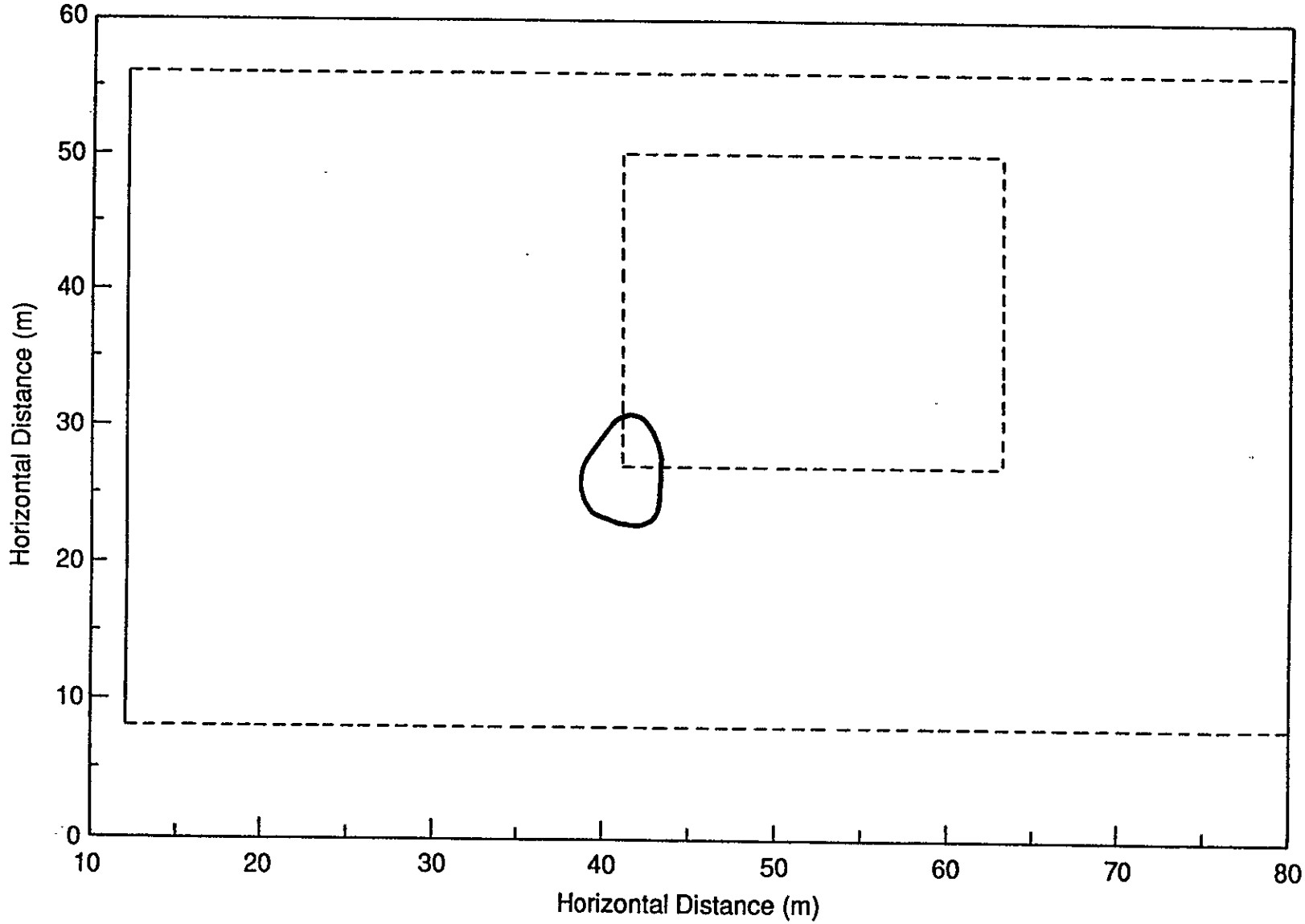

FIGURE 6.18. PORFLO-3 Simulation of the Horizontal Extent of the ^{137}Cs 1-μCi/L Isopleth Using Data from Field Measurements

150 days after the beginning of the leak. This simulation result compares favorably with observations in the dry wells adjacent to the tank, as reported by Routson et al. (1979). The horizontal plume dimension of 5 to 10 m also compares favorably with dimensions reported by Routson et al. (1979). Extension of the simulation through 1990 produced very little change in the configuration of the plume relative to its configuration about 65 days after the beginning of the leak. The simulation does not show any redistribution or reduction in the plume with time, probably a result of the high sorption and long half-life of ^{137}Cs.

7.0 CONCLUSIONS

The release of large quantities of fluid and contaminants from the 241-T-106 single-shell waste-storage tank in the 200-West Area of the Hanford Site was analyzed using a three-dimensional numerical model, PORFLO-3 Version 1.0. The analysis was made to calibrate model simulations to field measurements of the contaminant plumes for two radionuclides, ruthenium-106 and cesium-137. The release occurred during a period of 52 days in the summer of 1973. For purposes of the simulation, contaminant release was assumed to occur at a uniform rate during the period of release. The tank itself was assumed to be impermeable, except for a small break at the southwest end of the base where the leak occurred. Soil properties for the simulations were estimated, based on data contained in a catalogue of Hanford Site soil properties.

The model was calibrated to field measurements of the plume from 1973. For ^{106}Ru, the most mobile constituent, a reduction of the saturated hydraulic conductivity used in the initial set of simulations resulted in a plume configuration that closely approximated the measured configuration. Considering that the hydraulic conductivity used initially was for water, but that the leaked liquid was more viscous than water, this reduction in hydraulic conductivity appears reasonable.

Using the calibrated model, the plume measured in 1978 for ^{106}Ru was not approximated by the simulation. The plume measured in 1978 indicated that several meters of migration of the 1-μCi/L isopleth of ^{106}Ru occurred in several dry wells after 1973. The simulation, however, indicated a significant spreading of the plume in both the horizontal and the vertical direction since 1973. This result appears to be the consequence of the large amounts of ruthenium that leaked from the tank. Adjustment of the inventory may result in a better simulation approximation of the plume measured in 1978. Additional explanations may include the use of non-site-specific soil properties in the model and real or potential errors in measured data. Measurements of soil properties and the current extent of the plume are needed to resolve these questions.

The ^{137}Cs plume was approximated using a reasonable Kd in the simulations. The simulation results indicate that the plume penetrated only several meters below the base of the tank and became essentially stationary within about a month after the tank was pumped out, stopping the leak.

In the absence of information on soil properties specific to the T-106 tank site, Hanford Site soil properties were used. The simulation results approximate the measured ^{106}Ru and ^{137}Cs plumes with only minor adjustments of the soil property parameters, while keeping the contaminant source terms fixed. For future assessments, however, the use of soil properties measured at the T-106 tank site is recommended.

Preliminary simulation results indicate that, for the first 150 days, convection was the dominant transport phenomenon and the plume migration was governed by the large volume of the leak, rather than by the rate of infiltration of meteoric water from the surface. At later simulation times, reduction in the extent of the ^{106}Ru plume by radioactive decay was readily evident.

A saturated hydraulic conductivity on the order of 1×10^{-2} m/day for the stratigraphic units with relatively low hydraulic conductivities beneath the tank restricts, but does not appear to contain, downward migration of ^{106}Ru.

Several factors were not incorporated into the analysis. The thermal and viscosity effects of the liquid waste and active two-phase flow in the unsaturated zone were not included. The uncertainty introduced by not considering these factors is probably small relative to the lack of site-specific moisture retention properties. The PORFLO-3 code does not account for hysteresis in the soil-moisture characteristic curves. Hysteresis could have a significant impact on the movement of the liquid waste plume. Measurement of imbibition and drainage properties of at least the major soil horizon beneath the T-106 tank should be incorporated into plans for site characterization. These data may be significant in understanding the fate of plumes in the unsaturated zone, and plans for their collection should provide the impetus for code modifications to incorporate hysteresis.

Data on contaminant plumes in the vadose zone are rare. Consequently, the 241-T-106 leak data provided a rare opportunity to test the capabilities of the PORFLO-3 computer code. The PORFLO-3 code used for this analysis incorporates a complex set of equations for water flow, heat transfer, and mass transport. Its application to the 241-T-106 leak data, as discussed in this report, suggests that the code would be useful in helping to delineate and predict potential future movement of contaminant plumes from other sources at the Hanford Site, such as cribs and trenches.

THIS PAGE INTENTIONALLY
LEFT BLANK

8.0 REFERENCES

Ames, L. L., and D. Rai. 1978. Radionuclide Interactions With Soil and Rock Media, Volume 1. EPA 520/6-78-007, Environmental Protection Agency, Washington, D.C.

Atlantic-Richfield Hanford Company (ARHCO). 1973. 241-T-106 Tank Leak Investigation. ARH-2874, Atlantic Richfield Hanford Company, Richland, Washington.

Atomic Energy Commission (AEC-RL). 1973. Report on the Investigation of the 106-T Tank Leak at the Hanford Reservation, Richland, Washington. TID 26431, AEC-RL, Richland, Washington.

Bjornstad, B. N. 1983. Suprabasalt Stratigraphy Within and Adjacent to the Reference Repository Location. SD-BWI-DP-039, Rockwell Hanford Operations, Richland, Washington.

Coles, D. G., and L. D. Ramspott. 1982. "Migration of Ruthenium-106 in a Nevada Test Site Aquifer: Discrepancy Between Field and Laboratory Results." Science 215:1235-1236.

Evans, J. C., D. I. Dennison, R. W. Bryce, P. J. Mitchell, D. R. Sherwood, K. M. Krupka, N. W. Hinman, E. A. Jacobson, and M. D. Freshley. 1988. Hanford Site Ground-Water Monitoring for July Through December 1987. PNL-6315-2, Pacific Northwest Laboratory, Richland, Washington.

Fecht, K. R., and W. H. Price. 1977. Granulometric Data 241-T Tank Farm Monitoring Well Sediments. RHO-LD-19, Rockwell Hanford Operations, Richland, Washington.

Gee, G. W. 1987. Recharge at the Hanford Site: Status Report. PNL-6403, Pacific Northwest Laboratory, Richland, Washington.

Gillette, R. 1973. "Radiation Spill at Hanford: The Anatomy of an Accident." Science 181:728-730.

Isaacson, R. E. 1982. Supporting Information for the Scientific Basis for Establishing Dry Well Monitoring Frequencies. RHO-RE-EV-4 P, Rockwell Hanford Operations, Richland, Washington.

Jensen, E. J., S. P. Airhart, M. A. Chamness, T. J. Gilmore, D. R. Newcomer, and K. R. Oster. 1989. 40 CFR 265 Interim-Status Ground-Water Monitoring Plan for the Single-Shell Tanks. WHC-SD-EN-AP-012, Westinghouse Hanford Company, Richland, Washington.

Last, G. V., and B. N. Bjornstad. 1989. Revised Ground-Water Monitoring Plan for the 200 Areas Low-Level Burial Grounds. PNL-6902, Pacific Northwest Laboratory, Richland, Washington.

Last, G. V., B. N. Bjornstad, M. P. Bergeron, D. W. Wallace, D. R. Newcomer, J. A. Schramke, M. A. Chamness, C. S. Cline, S. P. Airhart, and J. S. Wilbur. 1989. Hydrogeology of the 200 Areas Low-Level Burial Grounds - An Interim Report. PNL-6820, Vol. 1, Pacific Northwest Laboratory, Richland, Washington.

Murthy, K. S., L. A. Stout, B. A. Napier, A. E. Reisenauer, and D. K. Landstrom. 1983. Assessment of Single-Shell Tank Residual Liquid Issues at Hanford Site, Washington. PNL-4688, Pacific Northwest Laboratory, Richland, Washington.

Philip, J. R., J. H. Knight, and R. T. Waechter. 1989. "Unsaturated Seepage and Subterranean Holes: Conspectus, and Exclusion Problem for Circular Cylindrical Cavities." Water Resources Research 25(1):16-28.

Price, W. H., and K. R. Fecht. 1976. Geology of the 241-T Tank Farm. ARH-LD-135, Atlantic Richfield Hanford Company, Richland, Washington.

Routson, R. C., W. H. Price, D. J. Brown, and K. R. Fecht. 1979. High-Level Waste Leakage from the 241-T-106 Tank at Hanford. RHO-ST-14, Rockwell Hanford Operations, Richland, Washington.

Runchal, A. K., and B. Sagar. 1989. PORFLO-3: A Mathematical Model for Fluid Flow, Heat, and Mass Transport in Variably Saturated Geologic Media, Users Manual, Version 1.0. WHC-EP-0041, Westinghouse Hanford Company, Richland, Washington.

Sagar, B., and A. K. Runchal. 1989. PORFLO-3: A Model for Fluid Flow, Heat, and Mass Transport in Variably Saturated Fractured or Porous Media - Theory Manual. WHC-EP-0042, Westinghouse Hanford Company, Richland, Washington.

Sewart, G. H., W. T. Farris, D. G. Huizenga, A. H. McMakin, G. P. Streile, and R. L. Treat. 1987. Long-Term Performance Assessment of Grouted Phosphate/Sulfate Waste From N Reactor Operations. PNL-6152, Pacific Northwest Laboratory, Richland, Washington.

Tallman, A. M., K. R. Fecht, M. C. Marratt, and G. V. Last. 1979. Geology of the Separation Areas, Hanford Site, South-Central Washington. RHO-ST-23, Rockwell Hanford Operations, Richland, Washington.

Thurman, J. M. 1989. Tank Farm Surveillance and Waste Status Summary Report for December 1988. WHC-EP-0182-9, Westinghouse Hanford Company, Richland, Washington.

U.S. Department of Energy (DOE). 1987. Final Environmental Impact Statement, Disposal of Hanford Defense High-Level, Transuranic and Tank Wastes. DOE/EIS-0113, Vols. 1-5, U.S. Department of Energy, Washington, D.C.

U.S. Energy Research and Development Administration (ERDA). 1975. Final Environmental Statement, Waste Management Operations, Hanford Reservation. Two vols. ERDA-1538, National Technical Information Service, Springfield, Virginia.

THIS PAGE INTENTIONALLY
LEFT BLANK

DISTRIBUTION

No. of Copies

OFFSITE

12 DOE/Office of Scientific and Technical Information

2 DOE Office of Civilian Radioactive Waste Management
Forrestal Building
Washington, DC 20585
ATTN: S. Rousso, RW-10
R. Stein, RW-30

2 DOE Office of Defense Waste & Transportation Management
GTN
Washington, DC 20545
ATTN: K. A. Chacey, DP-123
T. B. Hindman, DP-12

4 DOE Office of Remedial Action & Waste Technology
GTN
Washington, DC 20545
ATTN: J. E. Baublitz, NE-20
J. A. Coleman, NE-24
T. W. McIntosh, NE-24
H. F. Walter, NE-24

3 DOE Idaho Operations Office
550 Second Street
Idaho Falls, ID 83401
ATTN: C. R. Enos
M. W. Shupe
J. E. Solecki

C. S. Abrams
Argonne National Laboratory
P.O. Box 2528
Idaho Falls, ID 83401

R. G. Baca
EG&G, Inc.
2151 North Blvd.
Idaho Falls, ID 83415

No. of Copies

J. W. Bartlett
The Analytic Sciences Corporation
55 Walkers Brook Drive
Reading, MA 01867

3 Battelle Memorial Institute
Project Management Division
505 King Avenue
Columbus, OH 43201
ATTN: W. A. Carbeiner
R. A. Nathan
Technical Library

J. R. Berreth
Westinghouse Idaho Nuclear Co., Inc.
P.O. Box 4000
Idaho Falls, ID 83401

W. Brewer
Office of High-Level Nuclear Waste Management
Washington State Department of Ecology
Mail Stop PV-11
Olympia, WA 98504

W. J. Brumley
DOE Savannah River Operations Office
P.O. Box A
Aiken, SC 29801

G. S. Campbell
Agronomy Department
Washington State University
Pullman, WA 99164

A. T. Clark
Division of Fuel Material Safety
Nuclear Regulatory Commission
Washington, DC 20555

No. of Copies

G. A. Dinwiddie
U.S. Geological Survey
12201 Sunrise Valley Drive
Reston, VA 22092

6 E. I. du Pont de Nemours Company
Savannah River Laboratory
Aiken, SC 29801
ATTN: R. G. Baxter
M. D. Boersma
J. G. Glasscock
J. R. Knight
M. J. Plodinec
C. T. Randall

J. Fischer
Low-Level Radioactive Waste Program
U.S. Geological Survey
Water Resources Division
12201 Sunrise Valley Drive
Reston, VA 22092

F. T. Fong
DOE San Francisco Operations
1333 Broadway
Oakland, CA 94612

W. T. Goldston
DOE Savannah River Operations Office
P.O. Box A
Aiken, SC 29801

T. E. Hakonson
Los Alamos National Laboratory
P.O. Box 1663
Los Alamos, NM 87545

D. Hillel
Department of Plant and Soil Science
12A Stockbridge Hall
University of Massachusetts
Amherst, MA 01003

No. of Copies

Dwight Hoxie
U.S. Geological Survey
P.O. Box 25046, MS 421
Lakewood, CO 80225

E. A. Jacobson
Desert Research Institute
P.O. Box 60220
Reno, NV 89506

E. A. Jennrich
EG&G Idaho
P.O. Box 1625
Idaho Falls, ID 83415

M. R. Jugan
DOE Oak Ridge Operations Office
P.O. Box E
Oak Ridge, TN 37830

W. A. Jury
Department of Soils
University of California at Riverside
Riverside, CA 92502

D. A. Knecht
Westinghouse Idaho Nuclear Company
P.O. Box 4000
Idaho Falls, ID 83403

D. Langmuir
Department of Chemistry and Geochemistry
Colorado School of Mines
Golden, CO 80401

E. Maestas
DOE West Valley Project Office
P.O. Box 191
West Valley, NY 14171

S. O. Magnuson
EG&G, Inc.
2151 North Blvd.
Idaho Falls, ID 83415

No. of
Copies

J. M. McGough
DOE Albuquerque Operations
Office
P.O. Box 5400
Albuquerque, NM 87115

Sheldon Meyers
Environmental Protection Agency
Office of Radiation Programs
(ANR-458)
401 M Street S.W.
Washington, DC 20460

S. P. Neuman
Professor of Hydrology
Department of Water Resources
Building 11
University of Arizona
Tucson, AZ 87521

T. J. Nicholson
U.S. Nuclear Regulatory
Commission
Div of Engineering Safety
MS NL-005
Washington, DC 20555

J. W. Nyhan
Los Alamos National Laboratory
P.O. Box 1663
Los Alamos, NM 87545

4 Oak Ridge National Loaboratory
P.O. Box Y
Oak Ridge, TN 37830
ATTN: W. D. Burch
R. T. Jubin
L. J. Mezga
D. W. Turner

D. T. Oakley, MS-J521
Los Alamos Scientific Laboratory
P.O. Box 1663
Los Alamos, NM 87544

E. O'Donnell
Nuclear Regulatory Commission
MS-NLS-260
Washington, DC 20555

No. of
Copies

U-Sun Park
SAIC
101 Convention Center Drive,
Suite 860
Las Vegas, NV 89109

K. Pruess
Earth Sciences Division
Lawrence Berkeley Laboratory
University of California
Berkeley, CA 94720

L. D. Ramspott
Lawrence Livermore National
Laboratory
University of California
P.O. Box 808
Livermore, CA 94550

J. Rensel
High-Level Waste Management
Washington State Department
of Ecology
Mail Stop Pu II
Olympia, WA 98504

A. D. Rodgers
Mail Stop 2411
EG&G Idaho
P.O. Box 1625
Idaho Falls, ID 83415

2 Sandia Laboratories
P.O. Box 5800
Albuquerque, NM 87185
ATTN: R. W. Lynch
Technical Library

P. A. Saxman
DOE Albuquerque Operations Office
P.O. Box 5400
Albuquerque, NM 87185

R. R. Seitz
EG&G, Inc.
2151 North Blvd.
Idaho Falls, ID 83415

No. of
Copies

R. Shaw
Electric Power Research
Institute
3412 Hillview Avenue
P.O. Box 10412
Palo Alto, CA 94304

M. J. Steindler
Argonne National Laboratory
9700 South Cass Avenue
Argonne, IL 60439

V. Stello
Office of the Executive
Director for Operations
Mail Station 17-G21
Nuclear Regulatory Commission
Washington, DC 20555

D. B. Stephens
Daniel B. Stephens & Associates
4415 Hawkins NE
Albuquerque, NM 87109

C. F. Tsang
Earth Sciences Division
Lawrence Berkeley Laboratory
University of California
Berkeley, CA 94720

S. Tyler
Desert Research Institute
P.O. Box 60220
Reno, NV 89506

J. S. Wang
Earth Sciences Division
Lawrence Berkeley Laboratory
University of California
Berkeley, CA 94720

E. P. Weeks
U.S. Geological Survey
Federal Center Mail Stop 413
Denver, CO 80225

No. of
Copies

5 Westinghouse Savannah River
Company
Savannah River Site
Aiken, SC 29801
ATTN: R. G. Baxter
M. D. Boersma 77341A
J. R. Knight 773A
M. J. Plodinec 773A
C. T. Randall 7042

4 West Valley Nuclear Services
Company
P.O. Box 191
West Valley, NY 14171
ATTN: R. R. Borisch
J. Buggy
J. M. Pope
R. A. Thomas

J. L. White, Chairman
Energy Research & Development
Authority
Empire State Plaza
Albany, NY 12223

P. J. Wierenga
Department of Soil and Water
Science
University of Arizona
Tucson, AZ 85721

I. J. Winograd
U.S. Geological Survey
National center - Mail Stop 432
Reston, VA 22092

No. of Copies

ONSITE

12 DOE Richland Operations Office

G. J. Bracken
J. J. Broderick
C. E. Collantes
C. R. DeLannoy
J. R. Hunter
A. J. Knepp
O. L. Olson
J. M. Peterson
G. W. Rosenwald
M. W. Shupe
J. J. Sutey
D. M. Wanek

25 Westinghouse Hanford Company

M. R. Adams
L. C. Brown
J. W. Cammann
M. P. Connolley
H. F. Daugherty
J. D. Davis
K. R. Fecht
V. W. Hall
C. H. Huang
R. L. Jackson
M. T. Jansky
K. N. Jordan
R. Khaleel
D. S. Landeen
R. E. Lerch
H. E. McGuire
S. J. Phillips
W. A. Price
R. E. Raymond
J. F. Relyea
J. C. Sonnichsen
N. R. Wing
D. D. Wodrich
R. D. Wojtasek
J. C. Womack

No. of Copies

57 Pacific Northwest Laboratory

N. J. Aimo
P. A. Beedlow
M. P. Bergeron
L. L. Cadwell
M. D. Campbell
J. W. Cary
C. R. Cole
P. G. Doctor
J. L. Downs
J. W. Falco
M. J. Fayer (2)
M. G. Foley
M. D. Freshley
G. W. Gee
M. J. Graham
K. R. Hanson
P. C. Hays
D. J. Holford
T. L. Jones
C. T. Kincaid
R. R. Kirkham
G. V. Last
S. O. Link
J. F. McBride
E. M. Murphy
R. W. Nelson
M. L. Rockhold
B. Sagar (5)
C. S. Simmons
R. L. Skaggs
J. L. Smoot (10)
J. D. Smyth
J. A. Stottlemyre
G. P. Streile
C. F. Voss
W. J. Waugh
J. Weber
R. E. Wildung
Publishing Coordination
Technical Report Files (5)

THIS PAGE INTENTIONALLY
LEFT BLANK